AECL EACL

CA9600059

AECL-11330

Numerical Simulations of Groundwater Flow and SoluteTransport in the Lake 233 Aquifer

Simulations numériques de l'écoulement des eaux souterraines et de la migration des solutés de l'aquifère du Lac 233

M.H. Klukas, G.L. Moltyaner

May 1995 mai

AECL

Numerical Simulations of Groundwater Flow and Solute Transport in the Lake 233 Aquifer

by

M.H. Klukas and G.L. Moltyaner

Environmental Research Branch
Chalk River Laboratories
Chalk River, Ontario, KOJ 1J0
1995 May

AECL-11330

EACL

Simulations numériques de l'écoulement des eaux souterraines et de la migration des solutés de l'aquifère du Lac 233

par

M.H. Klukas et G.L. Moltyaner

RÉSUMÉ

Dans le cadre du stockage des déchets de faible activité, on élabore dans la présente publication un modèle tridimensionnel numérique de l'écoulement de l'aquifère du Lac 233 situé sous la construction souterraine anti-intrusion (IRUS). Comme entrées de base du modèle, on se sert d'une distribution de la conductivité hydraulique de référence comprenant les unités stratigraphiques déterminantes et les estimations de la recharge provenant du Lac 233 calculées d'après les données de terrain. Ce modèle a été étalonné en fonction de la distribution connue de la charge hydraulique, de la trajectoire d'un panache de ^{90}Sr antérieur dans l'aquifère et des vitesses établies des eaux souterraines.

Un certain nombre d'expériences numériques réalisées à l'aide du modèle a montré que la recharge en provenance du Lac 233 et la conductivité hydraulique de l'unité stratigraphique principale constituent les paramètres clés qui déterminent l'écoulement. On peut conceptualiser l'aquifère comme un bassin en pente pour lequel les seules sources d'eau souterraine sont la recharge en provenance du Lac 233 et les précipitations. L'écoulement souterrain s'effectue entièrement en direction du marais Duke. La valeur étalonnée de la conductivité hydraulique de l'unité statigraphique principale concordait bien avec la valeur estimée de la conductivité hydraulique extraite des analyses de la classe granulométrique 250. Les estimations de la recharge du Lac 233 établies d'après ce modèle correspondent bien aux valeurs estimées établies d'après les études effectuées sur le terrain.

La migration du panache de ^{90}Sr a été surveillée sur une période de 40 années et on a dressé une carte de ce panache en 1961 et 1983. On réalise le calcul prévisionnel de la migration du panache de ^{90}Sr réel à l'aide du modèle analytique unidimensionnel de Cameron et Klute [1977] qui décrit l'échange d'ions à l'état d'équilibre et les processus de sorption chimique à l'état de non-équilibre. La validité d'une méthode de modélisation unidimensionnelle pour décrire la migration du ^{90}Sr dans le principal sens d'écoulement est illustrée par référence à l'analyse des essais aux traceurs réalisés à Twin Lake, à des simulations numériques et à des simulations réalisées à l'aide du code d'évaluation des performances SYVAC-GEONET. Les simulations unidimensionnelles effectuées à l'échelle locale et à celle du panache pour l'aquifère de Twin Lake indiquent qu'une méthode unidimensionnelle convient bien pour donner une description du transport lorsque la dispersion transversale est faible et que l'on connaît le sens principal de l'écoulement.

Les données de terrain indiquent que la libération du ^{90}Sr dans la zone saturée a eu lieu à la manière d'un rejet de masses de matière. On prend en compte un scénario figurant un rejet uniforme d'une durée d'une année pour faire les prédictions en matière de transport. Les résultats des simulations indiquent que l'on obtient la meilleure concordance entre les concentrations de ^{90}Sr simulées et observées lorsque l'on prend en compte des processus de sorption à l'état de non-équilibre. Si on a recours à un modèle de sorption linéaire à l'état d'équilibre pour décrire l'échange de masse de ^{90}Sr, on obtient des surestimations de la concentration de ^{90}Sr maximale.

Les travaux dont on fait état dans cette publication ont été financés par l'institut de recherches sur l'énergie atomique du Japon (JAERI) et par le programme de R et D du GPC : Groupe de travail n° 49, WPIR n° 4950C.

Recherche sur l'environnement
Laboratoires de Chalk River
Chalk River, Ontario K0J 1J0
Mai 1995

AECL-11330

AECL

Numerical Simulations of Groundwater Flow and Solute Transport in the Lake 233 Aquifer

by
M.H. Klukas and G.L. Moltyaner

ABSTRACT

A three-dimensional numerical flow model of the Lake 233 aquifer underlying the site of the proposed Intrusion Resistant Underground Structure (IRUS) for low level waste disposal is developed. A reference hydraulic conductivity distribution incorporating the key stratigraphic units and field estimates of recharge from Lake 233 are used as model input. The model was calibrated against the measured hydraulic head distribution, the flowpath of a historic ^{90}Sr plume in the aquifer and measured groundwater velocities.

A number of numerical experiments performed with the model showed that recharge from Lake 233 and the hydraulic conductivity of the main stratigraphic unit are key flow controlling parameters. The aquifer can be conceptualized as a sloped basin for which the only groundwater source is recharge from Lake 233 and precipitation. All groundwater discharge is to Duke Swamp. The calibrated value of the hydraulic conductivity of the main stratigraphic unit was in good agreement with the hydraulic conductivity estimated from 250 grain size analyses. Model based estimates of Lake 233 recharge are in good agreement with estimates from field studies.

The migration of the ^{90}Sr plume has been monitored over its 40 year history and the ^{90}Sr plume was mapped in 1961 and 1983. Transport predictions of the migration of the historic ^{90}Sr plume are made using the one-dimensional analytical model of Cameron and Klute [1977], describing equilibrium ion-exchange and non-equilibrium chemical sorption processes. The validity of a one-dimensional modelling approach for describing ^{90}Sr migration along the principal flow direction is illustrated by reference to analysis of the Twin Lake tracer tests, numerical simulations and simulations performed using the SYVAC-GEONET performance assessment code. The one-dimensional simulations performed at the local and plume scales for the Twin Lake aquifer show a one-dimensional approach is suitable for describing transport when transverse dispersion is small and the principal flow direction known.

AECL-11330

Field data indicate that the ^{90}Sr was released to the saturated zone as a slug release. A scenario describing a uniform release of duration one year is considered for the transport predictions made. Simulations results show best agreement between simulated and observed ^{90}Sr concentrations when non-equilibrium sorption processes are considered. Use of an equilibrium linear sorption model for describing the ^{90}Sr mass exchange results in overprediction of maximum ^{90}Sr concentration.

The work reported in the document was funded by the Japanese Atomic Energy Research Institute (JAERI) and COG R & D Program: Working Party No. 49, WPIR No. 4950C

Environmental Research Branch
Chalk River Laboratories
Chalk River, Ontario, KOJ 1J0
1995 May

AECL-11330

Table of Contents

List of Figures

1.0 INTRODUCTION

Three-dimensional numerical flow models have been successfully applied to describe the groundwater flow path and velocities defined by the large scale natural gradient tracer tests at the Twin Lake aquifer at AECL's Chalk River Laboratories (CRL), [Moltyaner et al. 1993].

In the present study, a numerical flow model is developed to describe the flow regime at an adjacent site, also known as the Lake 233 aquifer. The aquifer is the site of a 40-year-old ^{90}Sr plume dating back to a ^{90}Sr release to the aquifer in 1954 at the location of the Nitrate Plant. Plume migration studies have been carried out over a 40-year period and are reported in Parsons [1963] and Killey and Munch [1987]. Modelling studies to assess groundwater flow and transport at the site have been performed by Lafleur et al. [1985] who developed a three-dimensional regional flow model of the site. Two-dimensional flow and transport modelling at a smaller scale limited to the immediate region enveloping the ^{90}Sr plume was performed by Robertson et al. [1987].

More recent field studies have provided far more detailed characterization of aquifer stratigraphy and estimates of recharge to the aquifer from Lake 233. Aquifer stratigraphy is characterized on the basis of geologic borehole logs, sediment grain size distributions and measured groundwater velocities. Over 250 grain size analyses on sediments sampled at the site have been performed allowing for qualitative description of the aquifer stratigraphy and estimates of hydraulic conductivity of the major stratigraphic units on the basis of grain size distribution. Borehole dilution velocities provide an independent means of evaluating aquifer stratigraphy and hydraulic conductivity through Darcy's Law.

The available field data on aquifer stratigraphy, hydraulic conductivity and recharge to the aquifer are used to develop a conceptual model of the groundwater flow system. Three-dimensional numerical simulations for steady-state flow conditions are performed. The model is evaluated on its ability to describe the observed hydraulic head distribution, the flowpath of the ^{90}Sr plume and measured groundwater flow velocities. Steady-state flow simulations are justified as maximum seasonal variability in the hydraulic gradient at the site is generally less than 30% and no seasonal variability in horizontal groundwater flow direction has been observed. The three-dimensional numerical model is calibrated against the fall hydraulic head distribution which is representative of the annual average.

The ^{90}Sr plume at Lake 233 is the result of accidental liquid releases to the aquifer in 1954 [Killey and Munch, 1987]. During the early 1950s experiments were performed in reprocessing spent fuel from the CRL reactors. This work generated aqueous ammonium nitrate solutions containing mixed fission products and a pilot plant to decompose the ammonium nitrate and reduce solution volumes was operated in 1953 and 1954. An infiltration pit, excavated adjacent to the Nitrate Plant and partially filled with crushed limestone, was intended to receive inactive condensate from the plant's evaporators. Process upsets led to a release of fission products including ^{90}Sr to the infiltration pit. More than 90% of the release occurred during a two week period at the end of November in 1954.

The migration of the ^{90}Sr plume has been monitored over its 40-year history and the ^{90}Sr plume was mapped in 1961 and 1983. Transport predictions of the migration of the historic ^{90}Sr plume are made using the one-dimensional model of Cameron and Klute [1977] describing equilibrium ion-exchange and non-equilibrium chemical sorption processes. The validity of a one-dimensional approach for describing the ^{90}Sr migration along the mean flow direction is illustrated by reference to analysis of the Twin Lake tracer tests. Field data suggest a slug release of ^{90}Sr to the saturated zone of the aquifer and transport simulations are made for such a release.

2.0 SETTING AND GEOLOGY

The geology of the Lake 233 aquifer is similar to that present over most of the CRL site and consists primarily of a granitic gneiss bedrock unit overlain by compacted glacial till which in turn is overlain by unconsolidated materials [Killey and Munch, 1987]. The most predominant of these is sand, generally ranging from very fine to medium in grain size. Figures 1a and b show the Lake 233 drainage basin, adjacent area and the existing monitoring network. Lake 233 receives surface runoff from the exposed bedrock to its northeast as well as from precipitation. Lake 233 drains by seepage into the underlying sediments; annual total groundwater recharge from Lake 233 is estimated to be 23 3500 m^3/a [Welch et al., 1989]. Flow in the underlying aquifer is to the west and southwest and discharges to Duke Swamp which is drained by Duke Stream and Lower Bass Creek. Figure 2 shows the model domain and the flowpath of the ^{90}Sr plume. After recharge from Lake 233, the major source of recharge to the aquifer is from precipitation. Precipitation at CRL over the period 1963 to 1988 has averaged 83 cm/a. Approximately 50 cm/a is lost through evapotranspiration leaving 30 cm/a for groundwater recharge [Robertson and Barry, 1985].

A dense network of multilevel piezometers has been installed in the region studied and the hydraulic head distribution at the site has been monitored at regular intervals over a 10-year period. Figures 3a-c show watertable contours for the observed hydraulic head distributions from April 14, July 4 and September 12, 1989. The hydraulic head data collected on these dates are the most complete data sets for spring, summer, and fall seasons. Groundwater flow direction inferred from the watertable contours are in agreement with the ^{90}Sr plume flowpath. Figure 4 shows a cross-sectional profile in the vertical plane of the seasonal variability in the measured water table elevations at locations along the centreline of the ^{90}Sr plume axis before spring recharge. Seasonal variability in hydraulic head is highest at Lake 233 where water levels increase by up to one and a half metres over the period of spring runoff. Seasonal variability in hydraulic head decreases with distance towards Duke Swamp where maximum seasonal variability in hydraulic head is of the order of 20 cm. Figure 5 shows hydraulic head depth profiles at multi-level locations C-124 and C-89, located at 50 m and 375 m downstream of Lake 233, respectively. Vertical hydraulic gradients are generally small, with the exception of the immediate vicinity of Lake 233, for example at C-124, where significant vertical gradients exist across the sediments underlying the lake.

Figure 6 shows the bedrock topography. Groundwater flow at the site is driven by bedrock topography and the flowpath of the ^{90}Sr plume follows the maximum gradient of the bedrock topography. Saturated thickness of the aquifer is eight to ten metres (Figure 4).

Groundwater residence times in the aquifer have been estimated from borehole dilution velocities measured adjacent to the flowpath of the ^{90}Sr plume [Killey and Munch, 1987]. An arithmetic mean of the measured velocities of 0.37 m/d gives groundwater residence time for the 600 m flowpath from Lake 233 to Duke Swamp to be 4.4 years.

2.1 Aquifer Stratigraphy and Hydraulic Conductivity

Stratigraphic cross-sections show the stratigraphic units making up the aquifer and are developed on the basis of geologic borehole log information and the grain size distribution of sampled sands. A stratigraphic unit is a unit having similar hydrogeologic properties over a suitably large scale and for sandy aquifers such as the Lake 233 aquifer, stratigraphic units can be defined on the basis of sand grain size distribution. Sands at over 250 locations have been sampled and are classified on the basis of grain size distribution according to the Wentworth classification scheme. Sediment sequences are correlated from borehole to borehole and the stratigraphic units defined. Figure 7 shows locations for which stratigraphic cross-sections have been constructed. Figures 8 and 9 show stratigraphic cross-sections along lines C-D and A-B. These cross-sections are representative of the stratigraphy of the Lake 233 aquifer for which the general stratigraphic sequence is interstratified sands and silts underlying Lake 233 followed by progressively coarser sands. The sands underlying the interstratified sands and silts are defined by two stratigraphic units: one consisting predominantly of fine and very-fine sands and a second unit consisting of medium-fine and fine-medium sands.

Once the stratigraphic units have been defined, the hydraulic conductivity of the units can be estimated. Hydraulic conductivity can be estimated on the basis of measured velocities and hydraulic gradients from Darcy's Law or by means of empirical relations relating grain size distribution to hydraulic conductivity. Here, Hazen's empirical formula, which was successfully used to characterize the hydraulic conductivity distribution at the Twin Lake tracer test site by Pfleiderer and Moltyaner [1993] is used. Hazen's empirical relation is written, [Hazen, 1983]:

$$K_{Hazen} = Ad^2_{10} \quad [cm/s] \tag{1}$$

where K_{Hazen} represents the hydraulic conductivity in centimetres per second derived from d_{10}, the tenth percentile of the grain size distribution in millimetres. The coefficient A accounts for other sediment properties effecting hydraulic conductivity such as sorting and grain shape. Empirically, $A = 1.16$ for well-sorted sand with $d_{60}/d_{10} \leq 5$.

Within a stratigraphic unit there is some variability in hydraulic conductivity due to spatial variability in the grain size distribution. Investigations at the Twin Lake site showed that within a single stratigraphic unit, grain size derived hydraulic conductivity logs could be correlated from well to well to develop a geometric model of the detailed hydraulic conductivity structure [Pfleiderer and Moltyaner, 1993]. Variability in the grain size derived hydraulic conductivity within the stratigraphic unit was of the order of 30%. The geometric model of the hydraulic conductivity structure is closely correlated to the spatial structure derived from the tracer test derived velocity field. At the Lake 233 aquifer there is insufficient data for such an analysis because longitudinal spacing between monitoring wells is 40 to 50 m, compared to 1 m at the Twin Lake site, and the vertical resolution of the grain size data available is much, 15 cm compared to 3 cm. Instead, for the Lake 233 aquifer a single average hydraulic conductivity is estimated for the individual stratigraphic units on the basis of the grain size distributions of the sediment samples making up the unit. This is valid provided that the grain size derived hydraulic conductivities for a given stratigraphic unit follow a normal distribution. For example, the average hydraulic conductivity of the fine-medium and medium-fine stratigraphic unit was obtained by combining the grain size derived conductivities of all fine-medium and medium-fine sands in a single population and calculating their arithmetic mean.

Table 1 lists the mean *(μ)* and standard deviation *(σ)* of the Hazen derived hydraulic conductivities for the fine-medium and medium-fine and fines and very fines stratigraphic units. Figure 10 shows the histograms of the Hazen-derived hydraulic conductivities for the stratigraphic units along with the associated normal distribution curves superimposed. The histograms of the Hazen-derived conductivities for both stratigraphic units approximate a normal distribution and the calculated mean hydraulic conductivities for these units can be used to estimate an average hydraulic conductivity.

No Hazen-derived estimate of the hydraulic conductivity of the interstratified sand and silt unit has been made, as Hazen's empirical relationship is not valid for fine silts (Hazen, 1893). Information from the geologic borehole logs suggest the unit is fairly heterogeneous having increasing permeability with distance from Lake 233.

Table 1: Hazen-Derived Hydraulic Conductivity of Stratigraphic Units

	Stratigraphic Unit	No. of Samples	Hydraulic Conductivity	
			μ *[cm/s]*	σ *[cm/s]*
	Fine-Medium and Medium - Fine	98	2.1E-02	1.03E-02
	Fines and Very Fines	154	8.65E-03	5.65E-03

Darcy velocities were measured through 15 borehole dilution tests along the cross section C-D providing vertical velocity profiles at five wells. The measured groundwater velocities provide an independent means of evaluating hydraulic conductivities through use of Darcy's Law. The measured groundwater velocities support the stratigraphic model estimated from the grain size distributions. Slower velocities are measured in the interstratified sands and silts, faster velocities in the more permeable underlying stratigraphic units. The hydraulic conductivity of the sands estimated from the Darcy velocities using Darcy's Law is comparable to that estimated from grain size analysis. All estimates lie within a factor of two of each other and for the most part, borehole dilution-derived and grain size-derived conductivities differ by less than 30%. Figure 11 shows vertical profiles at locations where Hazen-derived and borehole dilution velocity-derived conductivities are available.

The aquifer stratigraphy developed here is used as a basis for the conceptualization of the hydraulic conductivity distribution used in the flow simulations. Grain size-derived values of the hydraulic conductivity for the stratigraphic units are used as reference values for comparison against the estimates from the model calibration.

2.2 Conceptual Hydraulic Conductivity Distribution of the Lake 233 Aquifer for Flow Modelling

The hydraulic conductivity distribution of the Lake 233 aquifer used for flow modelling is conceptualized as three units. The sands underlying the interstratified sands and silts are treated as a single unit labelled K_1. This unit includes both the fine-medium and medium-fine and the fine and very fine stratigraphic units of the stratigraphic model described in Section 2.1. The interstratified sands and silts are treated as two units, K_2 and K_3, to describe the increasing permeability of this unit as observed from borehole logs with distance from Lake 233. Figure 12 shows a vertical cross-section of the model hydraulic conductivity distribution along the longitudinal axis of the model domain. Lateral variability in the hydraulic conductivity is small and is not considered.

Initial hydraulic conductivities of the units are based on the calibrated model reported in Lafleur et al., [1985] and are listed in Table 2. For the first simulations, the variability in the hydraulic conductivity of the interstratified sands and silts were not considered and a single conductivity was assigned to units K_2 and K_3. The ratio of the horizontal to vertical conductivity of the sandy unit (K_1) is taken to be three and is based on permeameter measurements of the vertical hydraulic conductivity of sands at the Twin Lake site [Killey and Moltyaner, 1988]. For the interstratified sands and silts the ratio of horizontal (K_x) to vertical conductivity (K_z) is assumed to be one order of magnitude greater than for the sands, owing to the effect of stratification in the horizontal plane.

Table 2: Hydraulic Conductivity Distribution for Initial Flow Simulations

	Hydraulic Conductivity (cm/s)		
Conductive Unit	Horizontal	Vertical	Ratio K_x/K_z
K_1	4.5E-03	1.5E-03	3
K_2	4.5E-04	1.5E-05	30
K_3	4.5E-04	1.5E-05	30

3.0 MATHEMATICAL MODEL OF FLOW THROUGH POROUS MEDIA

The governing equation describing fluid flow through saturated porous media is:

$$\frac{\partial}{\partial x_i}\left\{ K_{ij} \frac{\partial h}{\partial x_j} \right\} = S\frac{\partial h}{\partial t} \qquad (2)$$

where $x_i = x_1, x_2, x_3$, are the spatial coordinates that follow the principal directions of the hydraulic conductivity tensor K_{ij}, $h = h(x_1, x_2, x_3)$ is the hydraulic head, S is the storativity and $i,j = 1,2,3$. Under steady-state conditions the right hand term goes to zero. Boundary conditions specified are of the usual Dirichlet (constant head) and Neuman (specified flux) type. Flow simulations were performed using the thee-dimensional finite element flow code FLOW3D, developed at the Centre for Groundwater Research of the University of Waterloo. Details of the procedure for solving Equation (2) are given in Molson [1988]. Following the calculations of the hydraulic heads, the linear groundwater flow velocities are calculated using the Darcy equation in the form:

$$v = \frac{-K_{ii}}{n} \frac{\partial h}{\partial x_i} \qquad (3)$$

where n is the porosity.

4.0 CONCEPTUAL MODEL OF THE GROUNDWATER FLOW SYSTEM

Key parameters controlling groundwater flow in the aquifer are recharge from Lake 233 and precipitation, the hydraulic conductivity distribution and bedrock topography. Hydraulic head

at the discharge zone is controlled by hydraulic head at Duke Swamp. Hydraulic head upstream of the discharge zone is controlled by recharge to the aquifer from Lake 233 and precipitation, and the hydraulic conductivity distribution of the aquifer. The development of the conceptual model involves specifying boundary conditions and aquifer parameters that best approximate the measured aquifer parameters and natural boundaries of the groundwater flow system. The region modelled is centred about the flowpath of the ^{90}Sr plume which represents a long-term average of the regional flowpath. The model domain shown in Figure 2 includes the main areas of recharge and discharge from the site, Lake 233 and Duke Swamp, and covers an area of 250 m by 600 m. The upstream boundary coincides with the outcropping bedrock along the northeastern edge of Lake 233. The downstream boundary of the model domain borders on Duke Swamp. The bottom boundary represents the interface between the major sandy unit and the underlying bedrock till surface which was estimated from borehole log data. The top boundary of the model domain is defined by the watertable that lies within the interstratified sand/silt layer. The depth of the modelled domain ranges from eight to ten metres.

4.1 Aquifer Recharge

Groundwater recharge from Lake 233 to the entire underlying aquifer is estimated to be 233 500 m^3/a [Welch et al., 1989]. The model domain covers approximately 30% of the region receiving recharge from the lake. Assuming uniform recharge from Lake 233 to this area, we estimate recharge to the model domain to be 30% of the total recharge from Lake 233, giving annual recharge of 65 000 m^3/a. Annual recharge from precipitation is estimated to be 0.3 m/a. Recharge from precipitation is applied evenly over the region in the model domain downstream of Lake 233, with an area of 500 m by 250 m that gives total annual recharge from precipitation of 37 500 m^3/a. Total annual recharge to the model domain is the sum of groundwater recharge from Lake 233 and precipitation, 102 500 m^3/a.

For the domain considered watertable contours and the flowpath of the ^{90}Sr plume indicate that groundwater flow discharges into Duke Swamp. An independent test of the recharge estimate is made by calculating velocities at discharge to Duke Swamp and comparing these to groundwater velocities estimated from borehole dilution experiments at the site. Assuming all recharge into the model domain discharges to Duke Swamp, the calculated specific discharge is given by the relation:

$$S_D = R_T / A_D \qquad (4)$$

where R_T is the total recharge to the aquifer and A_D is the cross-sectional discharge area at Duke Swamp. For an annual recharge of 102 500 m^3/a and a cross-sectional discharge area

of 250 m width and 10 m depth the specific discharge is 41 m/a. The porosity of Chalk River sands is 40%, giving a pore velocity of 0.28 m/d. This compares favourably with the borehole dilution velocity measured in the aquifer of 0.37 m/d recorded in Killey and Munch [1987].

4.2 Boundary Conditions

In calibrating the model, various combinations of boundary conditions were considered. For the first simulations performed, constant head boundaries were specified on the four lateral sides of the domain and a no flow boundary was specified along the bedrock and watertable of the domain. Various combinations of boundary conditions were then applied to describe natural boundaries more accurately and to obtain better agreement between the observed and simulated hydraulic head distributions. Recharge from Lake 233 and precipitation were incorporated into the model with recharge rates estimated from field data.

5.0 MODEL CALIBRATION

The model was calibrated for steady-state conditions against the measured September 1989 hydraulic head data. The September 1989 hydraulic head data were chosen for the completeness of the data set and because fall hydraulic heads are most representative of the annual mean hydraulic head distribution. Calibration was performed by adjusting boundary conditions and the hydraulic conductivities assigned to the units K_1, K_2 and K_3. First simulations were performed for the hydraulic conductivity distribution and boundary conditions described in section 2.2 and 4.2. The specified heads on the lateral boundaries correspond to the September 1989 hydraulic heads at the boundary locations. No vertical variability in hydraulic head along the boundaries was considered. Figure 13 shows the simulated hydraulic head contours along with the observed water levels at locations near the flowpath of the ^{90}Sr plume. The greatest difference between the simulated and observed hydraulic heads is seen just downstream of Lake 233 with the simulated hydraulic head underestimating the observed head by up to one metre.

Boundary conditions were then modified and recharge from precipitation and Lake 233 incorporated into the model. It was found that the region modelled could be conceptualized as a basin closed on all sides except at the discharge zone to Duke Swamp. For this conceptualization the only sources of recharge to the aquifer are infiltration from Lake 233 and precipitation. The hydraulic head at the discharge zone is controlled by Duke Swamp. The upgradient boundary is treated as a no flow boundary because the boundary coincides with the outcropping bedrock to the northeast of Lake 233 and is essentially a groundwater divide. The lateral boundaries along the longitudinal axis of the domain are approximately parallel to the observed groundwater flowpath for which transverse flow is negligible and are also treated as no flow boundaries. The downgradient boundary at Duke Swamp was maintained as a constant head boundary allowing for discharge from the domain. Figure 14

shows a schematic of the boundary conditions and recharge rates applied for the calibrated model.

Groundwater recharge from Lake 233 into the model domain estimated to be 65 000 m^3/a was accounted for by applying a recharge rate of 2.52 m/a over an area of 250 m by 100 m at the northeast end of the model domain coinciding with the location of Lake 233. Recharge of 0.3 m/a was applied over the remainder of the model domain to account for recharge from precipitation. The described boundaries are believed to be an accurate representation of the natural boundaries of the system.

Further calibration was limited to calibration of the hydraulic conductivity distribution. This was performed through a number of iterations. The increasing hydraulic conductivity of the interstratified sand and silt layer with distance from Lake 233 was accounted for and the hydraulic conductivity of the main sandy unit, K_1, was increased by a factor of three to 1.35E-02 cm/s. Table 3 lists the calibrated hydraulic conductivities of the three units used to characterize the hydraulic conductivity distribution, K_1, K_2 and K_3. Table 4 lists the value of the Hazen-derived mean values of the two stratigraphic units, fine-medium and medium-fine and fines and very fines, making up the model hydraulic conductivity unit K_1. The calibrated hydraulic conductivity of this unit lies between the mean Hazen-derived conductivity of these two stratigraphic units.

Table 3: Calibrated Hydraulic Conductivity Distribution

	Hydraulic Conductivity [cm/s]	
Conductive Unit	Horizontal	Vertical
K_1	1.35E-02	4.5E-03
K_2	1.35E-03	4.5E-04
K_3	6.75E-04	2.25E-04

Table 4: Hazen-Derived Conductivity for the Major Stratigraphic Units of Conductive Unit K_1

	Hydraulic Conductivity [cm/s]
Fine-medium and medium-fine sands	μ = 2.1E-02 σ = 1.03E-02
Fine and very-fine sands	μ = 8.65E-03 σ = 5.65E-03

Figure 15 shows the simulated hydraulic head distribution at the surface and the measured hydraulic head at the piezometers nearest the centreline of the ^{90}Sr plume. Overall, agreement between the simulated and observed hydraulic head distribution is good. The greatest difference between simulated and observed hydraulic head is found immediately downstream of Lake 233. This is a region of high hydraulic gradients shown in observed water level profiles in Figure 4. Differences in simulated and measured hydraulic head in this region are of the order of 1 m. The difference in the simulated and observed hydraulic head is attributed to the complex stratigraphy and recharge patterns in the immediate vicinity of Lake 233 which are not described by the simple conceptualization of the groundwater flow system used for modelling. In comparison, agreement between simulated and measured hydraulic head data at the Twin Lake site was much better, with the root mean square error between the observed and simulated heads of 0.02 to 0.08 m for the nine wells at which comparisons were made [Moltyaner et al., 1993]. This is attributed to the simple groundwater flow system at the Twin Lake site; the hydraulic conductivity distribution at the site is much more uniform than at Lake 233 and recharge from infiltration is minimal. In addition, the model domain was an order of magnitude smaller than domain modelled here and more data were available for aquifer characterization.

Figure 16 shows the simulated hydraulic head potentials in the vertical plane along the longitudinal axis of the model domain at x = -70 m. Vertical gradients over most of the area are very small with the exception of the immediate vicinity of Lake 233 where seepage from Lake 233 through the interstratified sand/silt unit results in large vertical gradients. This is consistent with the conceptual model of the site where Lake 233 is the main source of recharge.

Figure 17 shows the velocity field for the calibrated model in the main conductive unit. Velocities are of the order of 0.30 to 0.40 m/d and approximate the mean flow path of the ^{90}Sr plume. Velocities are calculated using a porosity of 40%. The calculated velocities are in agreement with the mean value of 0.37 m/d for pore velocities estimated from borehole dilution techniques and a porosity of 40%.

5.1 Sensitivity Analysis

A sensitivity analysis was performed on the calibrated model to investigate the sensitivity of the simulated hydraulic head distribution to variability in the recharge rate and hydraulic properties. Three parameters are investigated: the groundwater recharge rate from Lake 233, the hydraulic conductivity of the main sandy unit, K_1, and the vertical anisotropy of the interstratified sand and silt unit. Model sensitivity to these parameters helps determine the effect of uncertainty in our parameter estimates on the model predictions. Figure 18 shows the effect of a 25% increase in recharge from Lake 233 on water levels at the site. Figure 19 shows the effect of a one order of magnitude decrease in vertical conductivity of the interstratified sand and silt unit. The effect of a 25% increase in the recharge from Lake 233 was to increase hydraulic head in the vicinity of Lake 233 by 1 m. The hydraulic head was relatively insensitive to an order of magnitude decrease in the vertical conductivity of the interstratified sand and silt layer.

Sensitivity of the hydraulic head to the conductivity of the main sandy unit K_1, was then evaluated. The calibrated value of the hydraulic conductivity of this unit, 1.35E-02 cm/s, lies between the estimated hydraulic conductivities of the stratigraphic units making up this unit; 2.1E-02 cm/s for the fine-medium and medium-fine sands and 8.65E-03 cm/s for the fine and very fine sands. The hydraulic conductivities of these two stratigraphic units are taken as the upper and lower bounds of the hydraulic conductivity of the main sandy unit. Figure 20 shows the watertable profiles along the longitudinal axis for both simulations. Figures 21 and 22 show the simulated hydraulic head contours in plan view. For a hydraulic conductivity of 8.65E-03 cm/s, hydraulic gradients are significantly greater than the observed; for hydraulic conductivity 2.1E-02 cm/s, hydraulic gradients are significantly less than the observed. The sensitivity of the simulated hydraulic head distribution to the hydraulic conductivity of this unit is explained by the fact that the bulk of the groundwater flow through the aquifer occurs through this unit. A change in conductivity of the major conductive unit results in a corresponding change in hydraulic gradients necessary to maintain the groundwater flow rates which are controlled by recharge to the aquifer from Lake 233 and precipitation. Average groundwater velocities corresponding to the low and high estimates of hydraulic conductivity for the two units are 0.34 and 0.55 m/d.

The sensitivity analysis shows that Hazen-derived conductivities can be used to characterize the hydraulic conductivity distribution. The sensitivity of the hydraulic head distribution to the hydraulic conductivity of this unit would also indicate that a more detailed characterization of the hydraulic conductivity distribution of the main sandy unit would result in more accurate simulations of the hydraulic head distribution.

6.0 THE APPLICABILITY OF A ONE-DIMENSIONAL APPROACH FOR MODELLING TRANSPORT

Transport processes in groundwater systems are three-dimensional by nature and the three-dimensional advection dispersion equation is generally required to describe these. However, when the principal flow direction is known and transverse dispersion is small compared to longitudinal dispersion the one-dimensional advection-dispersion model is often sufficient to describe transport. We illustrate the applicability of the one-dimensional approach for describing transport at the local and plume scales by reference to the analysis of the 1983 and 1987 tracer tests and the numerical simulations performed. We then describe the application of the one-dimensional advection dispersion equation incorporating parameters describing mass exchange processes to simulate the ^{90}Sr transport in the Lake 233 aquifer.

The 1983 and 1987 field scale tracer experiments at the Twin Lake site showed longitudinal dispersion along the mean flow path of the tracer to dominate over transverse dispersion [Moltyaner and Paniconi, 1984; Killey and Moltyaner, 1988; Moltyaner and Wills, 1991]. The dispersion process is described in detail in these papers. Transverse dispersion over the tracer flow path was minimal with little increase in the transverse dimensions of the plume. Fitted values of the transverse dispersivity were an order of magnitude less than the fitted values of the longitudinal dispersivity at the local scale. For such a small transverse dispersivity, it was shown that transport could be described using the one-dimensional advection-dispersion equation at the local and plume scales [Moltyaner and Wills, 1991]. The only transport parameters necessary to describe transport then are the velocity and dispersivity in the longitudinal direction along the mean flow path of the tracer.

The methodology for estimating transport parameters, velocity and dispersivity from the 1983 and 1987 tracer tests has been described in a number of papers [Moltyaner and Killey, 1988 a,b; Moltyaner, 1989; Moltyaner et al., 1991]. Local and Plume scale transport parameters are estimated by fitting the analytical solution to the one-dimensional advection dispersion equation to the observed concentration time data. The local scale refers to the scale at which the tracer concentration was measured and has a characteristic length of 0.1 m; the plume scale refers to the characteristic dimensions of the tracer plume and has dimensions of approximately 5 m for the 1987 Twin Lake tracer test [Moltyaner and Wills, 1991]. Local scale dispersion is the result of pore scale variability in the velocities. Plume scale dispersion is the result of larger scale variability in the velocity caused by stratigraphic contrasts as well as local scale dispersion within the individual strata. Local scale dispersivities are estimated by fitting the solution to the advection dispersion equation to the local scale breakthrough curves. Plume scale or full aquifer scale dispersivities are obtained by fitting to composite breakthrough curves where the composite breakthrough curve is obtained by averaging the time series of the local scale concentrations over the cross sectional area of the plume cross-section. Figures 23 and 24 show observed local and plume scale breakthrough curves for the 1983 tracer test and the fitted breakthrough curves. Longitudinal local scale dispersivity is of

the order of 0.01 m compared to fitted plume scale dispersivity of 0.3 m. Fitted values of longitudinal plume scale dispersivity are thus an order of magnitude greater than local scale dispersivity [Moltyaner and Killey, 1988].

Numerical simulations of the Twin Lake tracer tests show the limited effect of transverse dispersion on the plume transport. Three, one- and two-dimensional local scale and one-dimensional plume scale simulations of the 1983 Twin Lake Tracer test were performed. The three- and two-dimensional coupled flow and transport simulations are described in detail in [Moltyaner et al., 1993] and will only be briefly described here. The coupled flow and transport simulations were performed using the three-dimensional finite element flow code, FLOW3D, developed at the University of Waterloo [Molson, 1988], and the random walk based transport code, SLIM, developed at MIT, by Tompson, et al., [1987]. The simulations were carried out with grid orientation along the mean flow path of the tracer. Two-dimensional simulations were carried out in the vertical plane. Flow simulations were performed using the tracer test derived hydraulic conductivity distribution. Transport parameters specified are the velocity field from the flow simulation and the local scale longitudinal and transverse dispersivities. Comparison of the simulated breakthrough curves along the trajectory of the centre of mass of the tracer plume showed nearly identical concentration time curves for the two- and three-dimensional simulations over the first 25 m of the tracer test for which numerical simulations were performed, Figure 25. The simulations show the minimal effect of transverse horizontal dispersion on the tracer transport.

One-dimensional numerical simulations at the local scale have been performed to describe transport along the trajectory of the centre of mass of the Twin Lake tracer plume. Transport parameters are the longitudinal velocity and dispersivity. The initial condition for the transport simulation is the concentration distribution along the trajectory of the centre of mass at time 4.44 days. Figure 26 shows the one-dimensional local scale simulated and observed breakthrough curves at distances of 10, 15, 20 and 25 m from the injection well. One-dimensional numerical simulations at the plume scale were performed and simulation results compared to the plume scale averaged concentration time curves at distances of 20, 25 and 30 m west of the injection well. The initial condition for the simulation was the observed transverse averaged concentration profile at time 4.44 days. This was calculated by averaging local scale concentrations of the reconstructed plume at 4.44 days over the cross-sectional area transverse to the mean flow path of the tracer. The fitted plume scale dispersivity of 0.3 m is used in the simulations. Figure 27 shows the simulated and observed plume scale breakthrough curves. For both the local scale and plume scale simulations good agreement between the simulated and observed breakthrough curves is achieved.

One-dimensional local scale simulations of the 1983 tracer test have also been performed using the performance assessment code SYVAC-GEONET. The code is described in detail in Melnyk, [1994]. SYVAC-GEONET was developed to describe contaminant transport along a simplified set of pathways leading from an underground contaminant source to groundwater

discharge locations. Three dimensional contaminant transport is approximated by a three-dimensional network of one-dimensional transport segments connected in pairs by nodes. Flow and transport through the segments is one-dimensional. Segments are assigned constant physical and chemical properties so that analytical solutions may be used to describe contaminant transport along the segment. The basis for the model is the one-dimensional advection-dispersion equation including mass exchange and decay processes written as:

$$R_q \frac{\partial C_q}{\partial t} = D\frac{\partial^2 C_q}{\partial x^2} - U\frac{\partial C_q}{\partial x} - \lambda_q C_q + \lambda_{q-1} C_{q-1} \quad for\ q = 1, n \qquad (5)$$

where U is the linear groundwater velocity, D is the Dispersion Coefficient, R_q, retardation factor, λ_q is the decay constant, and C_q the groundwater concentration of nuclide q.

For application to the Twin Lake tracer test, only a single nuclide was considered, and the only processes are advection and dispersion. Analytical solutions to the advection-dispersion equation are provided in SYVAC-GEONET for various initial and boundary conditions. To describe transport at the Twin Lake site we use the analytical solution for a semi-infinite domain and specified mass flow rate on the input boundary. Local scale simulations of the 1983 Twin Lake tracer test are performed in the vertical plane over the first 20 m of the tracer test flow path. Eleven segments of 20 m length are used to describe tracer transport in the tracer occupied zone of the aquifer, one for each velocity zone identified from the tracer test. Simulations performed here are deterministic and utilize tracer test derived transport parameters. Transport parameters assigned to each segment are the velocities corresponding to the segment and the mean fitted longitudinal dispersivity of 0.01 m. The source term is the nuclide flow rate of units activity/time specified over time t describing the initial pulse from the tracer injection. Figure 28 shows simulated concentration-time curves at 20 metres from the source for elevations 142.74, 143.54 and 145.00 masl.

The one-dimensional numerical simulations of the Twin Lake tracer tests at the local and plume scales, as well as the simulations performed using the SYVAC-GEONET performance assessment code show the one-dimensional approach for describing transport when the principal flow direction is known and transverse dispersion is small relative to longitudinal dispersion. We use the same one-dimensional approach and incorporate parameters to describe ^{90}Sr mass exchange to simulate the ^{90}Sr plume migration at the Lake 233 site.

6.1 The Lake 233 ^{90}Sr Plume, Background and One-Dimensional Analytical Model for Predicting the ^{90}Sr Plume Migration

The historic ^{90}Sr plume at Lake 233 is the result of accidental liquid releases to the aquifer in 1954 [Killey and Munch, 1987]. During the early 1950s experiments were performed on

reprocessing spent fuel from the CRL reactors. This work generated aqueous ammonium nitrate solutions containing mixed fission products, and a pilot plant to decompose the ammonium nitrate and reduce solution volumes was operated in 1953 and 1954. An infiltration pit excavated adjacent to the Nitrate Plant, partially filled with crushed limestone, was intended to receive inactive condensate from the plant's evaporators. During process upsets, fission products including ^{90}Sr were released to the infiltration pit. More than 90% of the release occurred during a two week period at the end of November in 1954. A major nuclide in the solution was ^{90}Sr and the total estimated ^{90}Sr input to the aquifer is 26 to 37 TBq [Parsons, 1963].

The resulting ^{90}Sr plume has been mapped in 1961 and 1983 and the plume front advance monitored over the past 40 years. The most recent plume mapping in 1983 [Killey and Munch, 1987] yielded an inventory of 13.44 TBq, (28.2 TBq if decay corrected to 1954), in good agreement with the estimate by Parsons [1963]. The plume mapping in 1983 provided estimates of the ^{90}Sr inventory along transects perpendicular to the plume axis. Figure 29 shows the 1983 ^{90}Sr distribution with distance from the source. The centre of mass of the plume was calculated to be 95 m from the source in 1983.

The base of the infiltration pit was located approximately 7 to 8 m above the average water-table elevation. Field data suggest the ^{90}Sr migrated fairly rapidly from the infiltration pit to the saturated zone of the aquifer. One year after the release the plume front had advanced 80 m downstream of the infiltration pit. As well, the 1961 plume inventory indicates that the bulk of the released ^{90}Sr had entered the saturated zone by this time. The rapid migration of the ^{90}Sr through the unsaturated zone is attributed to competition for and occupation of sorption sites by the high concentrations of non-radioactive cations in the initial release with the most abundant non-radioactive cations being NH_4^+ from the ammonium nitrate solution and Ca^{2+} from the limestone in the infiltration pit.

Hydrogeochemical processes affect the migration of ^{90}Sr in groundwaters and several studies investigating mass exchange between ^{90}Sr groundwater and the soil matrix have been performed, for example, [Jackson and Inch, 1980; Champ et al., 1985; Killey et al., 1994]. The exchange between ^{90}Sr in solution and on solid occurs primarily by means of ion exchange and through slower chemical sorption onto iron and aluminum oxides on the sands. For CRL sands, approximately 60% of sorption occurs by ion exchange, and 30% by chemical sorption. Sorption by ion exchange is considered to occur very quickly and equilibrium is reached within hours. Sorption onto the aluminum and iron oxides is much slower and can take years to reach equilibrium. The one-dimensional model of Cameron and Klute [1977] considers both the equilibrium and non-equilibrium sorption and is applied here to describe the plume scale ^{90}Sr concentration distribution measured in the 1983 field study, Killey and Munch [1987]. The model assumes two types of sorption sites: sorption sites characterized by instantaneous mass exchange and sorption sites characterized by very slow mass exchange. Both sorption mechanisms are considered to be reversible and the non-

equilibrium sorption is described using a first order kinetic model, Eq. (6). Coupling surface reactions with the one- dimensional advection dispersion equation gives:

$$(1+R_3)\frac{\partial C}{\partial t} = D_L\frac{\partial^2 C}{\partial x^2} - v\frac{\partial C}{\partial x} - \frac{\rho_b}{n}\frac{\partial S_1}{\partial t}$$
$$\frac{\partial S_1}{\partial t} = R_1\frac{n}{\rho_b}C - R_2 S_1 \qquad (6)$$

where C is the liquid phase concentration, D the dispersion coefficient, v the velocity, R_1, R_2 and R_3 are the forward rate, reverse rate and equilibrium constant, respectively. S_1 is the concentration on the kinetic sites, ρ_b is the soil bulk density, and n the porosity.

The ratio of solute on the solid phase to solute in solution is given by the distribution coefficient. Two distribution coefficients are associated with the two-site kinetic model, one associated with the equilibrium sorption, the other with the non-equilibrium or kinetic sorption. The distribution constant associated with the kinetic sites, once equilibrium has been reached, is given by the relation [Moltyaner and Champ, 1987]:

$$K_{d1} = \frac{S_1}{C} = \frac{R_1 n}{R_2 \rho_b} \qquad (7)$$

where S_1 is the concentration associated with the kinetic sites and C the concentration in solution. The distribution coefficient for the equilibrium sorption is given by the relation:

$$K_{d2} = \frac{S_2}{C} \qquad (8)$$

where S_2 is the concentration on the 'instantaneous' equilibrium sites. The equilibrium constant R_3 given in Eq. (6) is the dimensionless form of the distribution coefficient in Eq. (8) and is equal to:

$$R_3 = \frac{\rho_b}{n}K_{d2} \qquad (9)$$

Total adsorption at equilibrium is:

$$S_{eq} = \frac{n}{\rho_b} \left(\frac{R_1}{R_2} + R_3\right) C \tag{10}$$

Cameron and Klute [1977] illustrate the effect of the forward and reverse rate constants on the transport predictions. The forward reaction rate constant R_1 describes sorption at kinetic sites, the reverse reaction rate constant R_2 describes desorption at these sites. For a large ratio of R_1/R_2 , non-equilibrium effects will be pronounced. With decreasing ratio R_1/R_2 , the transport predictions will approximate those of an equilibrium linear sorption model.

The analytical solution to the two-site kinetic model of Eq. (6), for a semi-infinite medium having initial and boundary conditions:

$$\begin{gathered} c(x, t)\,|_{t=0} = 0; \quad s(x, t)\,|_{t=0} = 0 \\ c(x, t)\,|_{x=\infty} = 0 \\ c(x, t)\,|_{x=0} = c_o\,\Phi(t) \end{gathered} \tag{11}$$

and continuous input function:

$$\Phi(t) = 1 \tag{12}$$

is given in Moltyaner and Champ [1987] and is:

$$\begin{aligned} f(x, t) = \frac{x}{2}\sqrt{\frac{(1 + R_3)}{\pi D}} \int_o^t Z^{-1.5} \exp \\ \left[-\frac{R_1 Z}{(1 + R_3)} - R_2(t - Z) - \frac{[x\,(1 + R_3) - v\,Z]^2}{4\,D\,(1 + R_3)\,Z}\right] \\ \cdot I_o\left(2\frac{\sqrt{R_1 R_2 (t - Z)}}{(1 + R_3)}\right) dZ \end{aligned} \tag{13}$$

To describe the ^{90}Sr release to the Lake 233 aquifer a constant concentration at the first type boundary is specified for duration t_o. The solution is found by superposition,

$$C(x, t) = c(x, t) - c(x, t-t_o) \quad for \quad t > t_o \tag{14}$$

where $C(x,t)$ is the ^{90}Sr concentration in solution at time t.

6.2 Transport Parameters

Transport parameters to be specified are the velocity, dispersion coefficient, distribution coefficient for equilibrium or short term sorption and the forward and reverse rate constants for the slower chemical sorption. Simulations used a mean flow velocity of 0.37 m/d estimated from the field studies. Plume scale dispersivity was assumed to be of the same magnitude as that estimated from the Twin Lake tracer experiments; a value of 0.1 m^2/d is used.

The most uncertainty lies in the parameters describing ^{90}Sr mass exchange. Killey and Munch, [1987] summarize available data on distribution coefficients estimated by various methods. Batch tests provide information on short term (equilibrium) sorption and give a log mean K_d of 7.9 mL/g. Long-term in situ distribution coefficients are estimated from the ^{90}Sr concentration in the contaminated sands and associated solution and provide a log mean of 12.9 mL/g. Distribution coefficients are also estimated from historical data on the movement of the ^{90}Sr plume. Given the position of the plume front, the retardation factor given by the velocity of the plume front relative to the average groundwater velocity is calculated and the distribution coefficient estimated from the relation:

$$K_d = \frac{n}{\rho_b} (R - 1)$$

$$R = \frac{V_{gr}}{V_{90_{SR}}} \tag{15}$$

where V_{gr} is the linear groundwater velocity and V_{90Sr} the velocity of the plume front. Plume front distribution coefficients range from 0.8 mL/g to 4.8 mL/g and increase linearly over time. Distribution coefficients have also been estimated from the movement of the centre of mass of the plume. These are up to an order of magnitude lower than those estimated from

the plume front and reflect the slow non-equilibrium sorption. The low plume front K_ds are in part explained by the fact that the plume front moves along the path of least resistance and reflect the lower limit of K_ds in the aquifer.

For the transport simulations, the distribution coefficient used to describe equilibrium sorption is that determined from batch tests, having value of 7.9 mL/g. For this value of distribution coefficient, we calculate an equilibrium constant R_3 of 31.6 from Eq. (9) using a porosity of 0.4 and a bulk density of 1.6 g/cm^3.

Two sets of reaction rate constants are considered to describe the chemical sorption. We use rate constants from calibration of the one-dimensional model of Cameron and Klute [1977] against a large scale field experiment, the ^{90}Sr plume migration over a 30 year period at an adjacent site on the CRL property [Killey et al., 1994]. We also use rate constants derived from column experiments reported in Moltyaner and Champ [1987]. The ^{90}Sr migration from the field experiment shows significant non-equilibrium effects: significant broadening of the plume and much slower movement of the centre of mass of the plume than would be expected if mass exchange was by equilibrium sorption alone. Calibration of transport parameters against the ^{90}Sr plume migration of the field experiment yielded values of forward and reverse rate constants of 6.0E-03/d and 2.0E-04/d [Killey et al., 1994]. The distribution coefficient associated with these rate constants is 7.5.

In comparison, the column experiments using ^{85}Sr reported in Moltyaner and Champ [1987], showed symmetric breakthrough curves indicating small non-equilibrium effects. The ratio of the forward to reverse rate constant obtained by fitting against the column elution curves was three, an order of magnitude less than from calibration against the field experiment data. For this second parameter set, we use the R_1/R_2 ratio derived from the column experiment, giving forward and reverse rate constants of 6.0E-03/d and 2.0E-03/d, respectively.

6.3 Source Term Modelling

The ^{90}Sr release to the aquifer is described in Section 6.1. As discussed, there is some uncertainty regarding the time required for the ^{90}Sr released to the infiltration pit to reach the saturated zone of the aquifer for which transport is modelled. We know that significant amounts of ^{90}Sr entered the aquifer within one year of the release because the plume front had moved 80 metres from the source in the first year. The 1961 plume mapping, seven years after the release, showed that the bulk of the ^{90}Sr released had entered into the aquifer at this time, making the upper bound for the time required for the ^{90}Sr to enter the saturated zone seven years. For the simulations we assume two release durations: a uniform release over a one-year period and a uniform release over a three-year period to the saturated zone of the aquifer.

6.4 Model Predictions

Strontium-90 activity distance profiles are calculated using the analytical solution given in Eq. (13) and the specified transport parameters for the two release scenarios. For the one-dimensional solution concentration units are ^{90}Sr activity in the fluid per unit length. We predict the ^{90}Sr activity profile for the time 28.5 years after the release, the time at which the 1983 plume mapping was performed. Total ^{90}Sr activity is calculated from the predicted ^{90}Sr activity in solution under the assumption that equilibrium has been reached for the slow mass exchange sorption and is calculated from the relation given in Moltyaner and Champ [1987]:

$$S_e = \left(\frac{R_1}{R_2} + R_3\right) c\frac{n}{\rho_b} + nc \qquad (16)$$

where S_e is the total ^{90}Sr activity per unit length and c is the ^{90}Sr activity in solution per unit length.

Figure 30 shows the predicted ^{90}Sr activity profiles for the one-year release scenario for both sets of rate constants along with the observed ^{90}Sr activity profile. Predicted ^{90}Sr activity profiles for a source term of three-year release duration are also shown in Figure 30 and are essentially identical to those for the one-year release duration.

The observed ^{90}Sr activity profile shows significant tailing associated with the non-equilibrium sorption and the ^{90}Sr profile was best described using the field derived rate constants R_1 and R_2. Strontium-90 predictions made using the rate constants derived from the column experiment do not describe the broadening of the plume and show a gaussian activity profile typical of the linear equilibrium sorption model. The predicted ^{90}Sr is narrower and the peak ^{90}Sr activity greater by a factor of five than the observed. Predictions show that an equilibrium sorption model will overpredict peak ^{90}Sr activity and underpredict plume spreading along the flowpath.

Figure 31 shows predicted ^{90}Sr concentration versus time curves at a location 110 m from the source for non-equilibrium and equilibrium sorption models. Although the ^{90}Sr concentration time curves predicted by the two models differ, the concentration time integral and, therefore, the total predicted dose to an individual from the two models is the same. When transport can be described using a one-dimensional model, the concentration time integral is given by the total activity released, divided by the flow rate; the total dose to an individual can be calculated from these parameters alone. The differences in predicted dose for the two models is only with respect to the time period over which the dose is received.

7.0 CONCLUSIONS

A three-dimensional numerical flow model is developed for the aquifer underlying the proposed site of the Intrusion Resistant Underground Structure. The model domain is oriented along the flow path of the historic ^{90}Sr plume in the aquifer. It is shown that the aquifer can be conceptualized as a rectangular basin closed on three sides and open only to discharge at Duke Swamp. All recharge to the aquifer is from Lake 233 and precipitation. Flow is simulated under steady-state conditions and the model was calibrated against the observed hydraulic head distribution from September 1989 and measured groundwater velocities. A sensitivity analysis showed the key parameters controlling flow in the aquifer to be recharge from Lake 233 and the hydraulic conductivity of the main sandy unit in the aquifer. Hydraulic conductivity of the main sandy unit is estimated from 250 grain size analyses. Recharge from Lake 233 has been estimated from water budget calculations for the aquifer. The calibrated values of recharge from Lake 233 and hydraulic conductivity of the main sandy unit are in agreement with the field based estimates. Flow in the main sandy unit of the aquifer follows an approximate straight line path from Lake 233 to the discharge zone. Average simulated groundwater flow velocities corresponding to upper and lower bounds of the hydraulic conductivity of this unit are 0.34 and 0.55 m/d.

Predictions of the ^{90}Sr plume migration were performed using the one-dimensional model of Cameron and Klute [1977], incorporating non-equilibrium sorption processes. The use of a one-dimensional model for describing the ^{90}Sr migration along the principal flow direction is justified on the basis of the limited transverse dispersion observed in the large-scale field tests carried out at the adjacent Twin Lake aquifer and the ^{90}Sr plume here. The one-dimensional numerical simulations of the Twin Lake tracer tests at the local and plume scales, as well as the Twin Lake simulations performed using the SYVAC-GEONET code, demonstrate the applicability of a one-dimensional approach to describe transport when transverse dispersion is small relative to longitudinal dispersion and the principal flow direction is known.

Input parameters to the model describing ^{90}Sr sorption processes are the distribution coefficient for equilibrium sorption and reaction rate constants for non-equilibrium sorption. The ^{90}Sr release to the aquifer was modelled as a uniform release of one-year duration. The distribution coefficient used in the model was that estimated from batch tests. The best agreement between predicted and observed ^{90}Sr plume profile was obtained using reaction rate constants for which non-equilibrium sorption effects were significant. Transport predictions showed that an equilibrium sorption model will overpredict peak ^{90}Sr concentrations. Total predicted dose to an individual, when transport is described by a one-dimensional model, is a function of total activity released and the groundwater flow rate, and is independent of the sorption model used to describe the ^{90}Sr transport.

8. ACKNOWLEDGEMENTS

Funding for this work was provided by the Japan Atomic Energy Research Institute (JAERI), the CANDU Owners' Group, and AECL.

9. REFERENCES

Cameron, D.R. and A. Klute. 1977. Convective-Dispersive Solute Transport with a Combined Equilibrium and Kinetic Adsorption Model, Water Resources Research, Vol. 13, No. 1, 183-188.

Champ D.R., G.L. Moltyaner, J.L. Young and P. Lapcevic. 1985. A Downhole Column Technique for Field Measurement of Transport Parameters, AECL-Report 8905.

Hazen, A. 1893. Some Physical Properties of Sand s and Gravels with Special Reference to Their Use in Filtration. Annu. Rep. Mass. Board of Public Health, 541-556.

Jackson, R.E., and K.J. Inch. 1980. Hydrogeochemical Processes Affecting the Migration of Radionuclides in a Fluvial Sand Aquifer at the Chalk River Nuclear Laboratories, NHRI Paper No. 7, Scientific Series No. 104, National Hydrology Research Institute, Inland Waters Directorate, Ottawa, Canada.

Killey, R.W.D., M.H. Klukas, J.L. Young, and G.L. Moltyaner. 1994. The Glass Block Experiment, 30 Years Later, AECL-Report, In Preparation.

Killey, R.W.D., and J.H. Munch. 1987. Radiostrontium Migration from a 1953-1954 Liquid Release to a Sand Aquifer, Water Poll. Res. J. Canada, 22 (1), 107-128.

Killey, R.W.D., and G.L. Moltyaner. 1988. Twin Lake Tracer Test: Setting, Methodology, and Hydraulic Conductivity Distribution, Water Resources Research, Vol. 24, No. 10, 1585-1612.

Lafleur, D.W., J.F. Pickens and R.W.D. Killey. 1985.Hydrogeologic Assessment of the 233 Lake Area: Calibration of a Three-Dimensional Groundwater Model, AECL-Report, TR-257.

Melnyk, T. 1994. Analysis and Specifications for the CC3 Geosphere Model - GEONET, AECL Report, AECL-11077, COG-94-101.

Molson, J.W.H. 1988. Three-Dimensional Numerical Simulation of Groundwater Flow and Contaminant Transport at the Borden Land fill, MSc. Thesis, University of Waterloo, Waterloo, Ontario.

Moltyaner, G.L. and D.R. Champ. 1987. Mass Transport in Saturated Porous Media: Estimation of Transport Parameters, AECL Report, AECL - 9610.

Moltyaner, G.L. and R.W.D. Killey. 1988a. Twin Lake Tracer Tests: Longitudinal Dispersion, Water Resources Research, Vol. 24, No. 10, 1613-1627.

Moltyaner, G.L. and R.W.D. Killey. 1988. Twin Lake Tracer Tests: Transverse Dispersion, Water Resources Research, Vol. 24, No.10, 1628-1637.

Moltyaner, G.L. 1989. Hydrodynamic Dispersion at the Local Scale of Continuum Representation, Water Resources Research, Vol. 25, No. 5, 1041-1048.

Moltyaner, G.L., M.H. Klukas, C.A. Wills, and R.W.D. Killey. 1993. Numerical Simulations of Twin Lake Natural-Gradient Tracer Tests: A Comparison of Methods, Water Resources Research, Vol. 29, No. 10, 3433-3452.

Moltyaner, G.L. and C. Paniconi. 1984. Migration of Radionuclides in Porous Media: Analysis of Experimental Data, AECL-Report, AECL-8254.

Moltyaner, G.L. and C.A. Wills. 1991. Local and Plume-Scale Dispersion in the Twin Lake 40- and 260-m Natural Gradient Tracer Tests, Water Resources Research, Vol. 27, No.8, 2007-2026.

Parsons, P.J. 1963. Migration From a Disposal of Radioactive Liquid in Sand s, Health Physics., Vol. 9, 38-42.

Pfleiderer S. and G.L. Moltyaner. 1993. The Use of Velocity and Conductivity Data for the Quantification of Heterogeneity: A Comparison, Water Resources Research, Water Resources Research, Vol. 29, No. 12, 4151-4156.

Robertson, D.E., M.P. Bergeron, D.A. Myers, K.H. Abel, C.W. Thomas, D.R. Champ, R.W.D. Killey, G.L. Moltyaner, and J.L. Young. 1987. Demonstration of Performance Modelling of a Low-Level Waste Shallow Land Burial Site: A Comparison of Predictive Radionuclide Transport Modelling versus Field Observations at the Nitrate Disposal Pit Site, Chalk River Nuclear Laboratories, NUREG/CR-4879, Volume 1, PNL -6175, U.S. Nuclear Regulatory Commission, Washington, D.C.

Robertson, E. and P.J. Barry. 1985. The Water and Energy Balances of the Perch Lake (1969-1980). Atmosphere-Ocean 23 (3), 238-253.

Tompson, A.F.B., E.G. Vomvoris, and L.W. Gelhar. 1987. Numerical Simulations of Solute Transport in Randomly Heterogeneous Porous Media: Motivation, Model Development and Application, Rep. UCID-2181, Lawrence Livermore Natl. Lab., Livermore, Calif.

Welch, J., D.R. Lee and R.W.D. Killey. 1989. Determination of Seepage Flux From Lake 233 to the Underlying Aquifer, AECL-Report, TR-470.

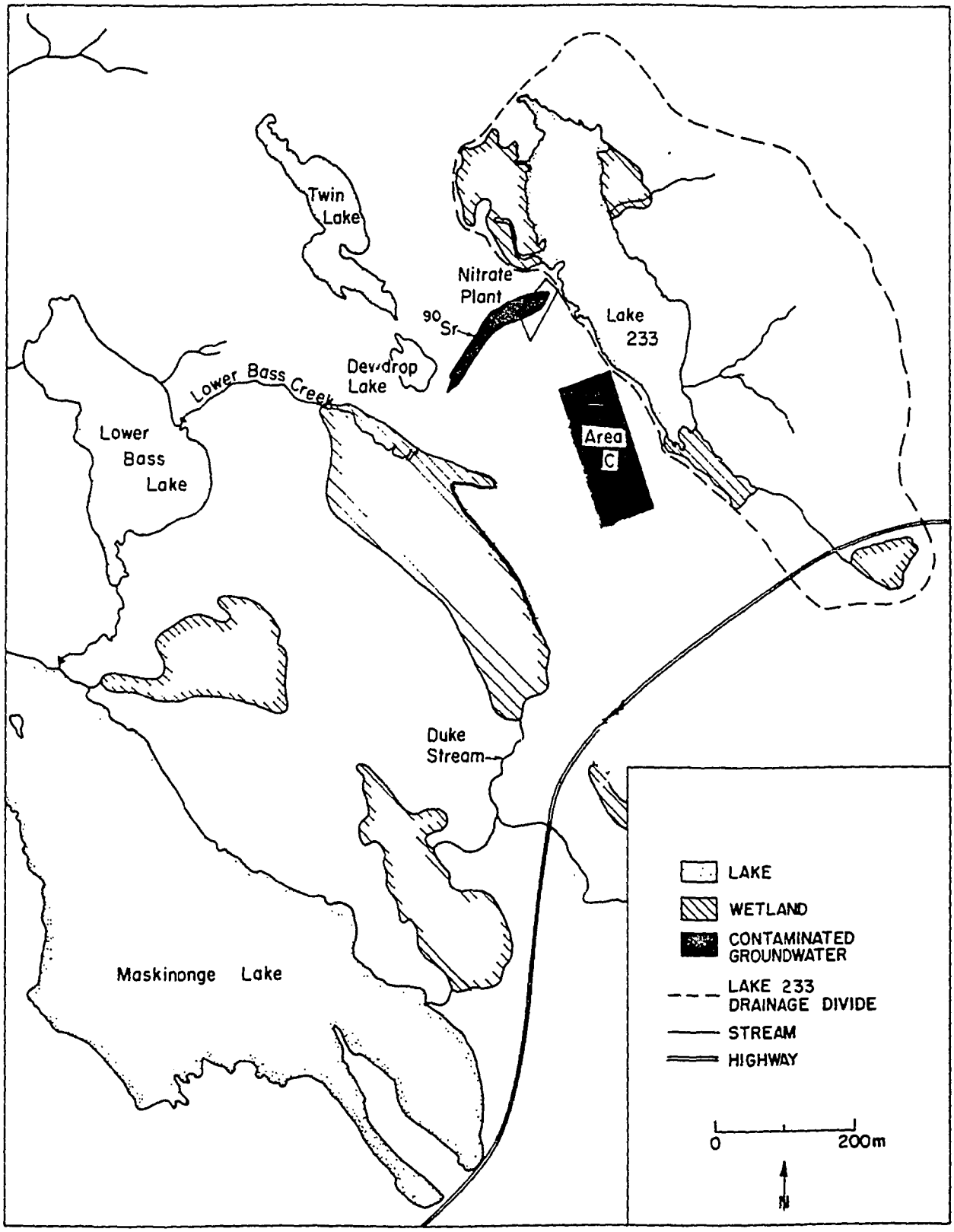

Figure 1a Plan view of the study area

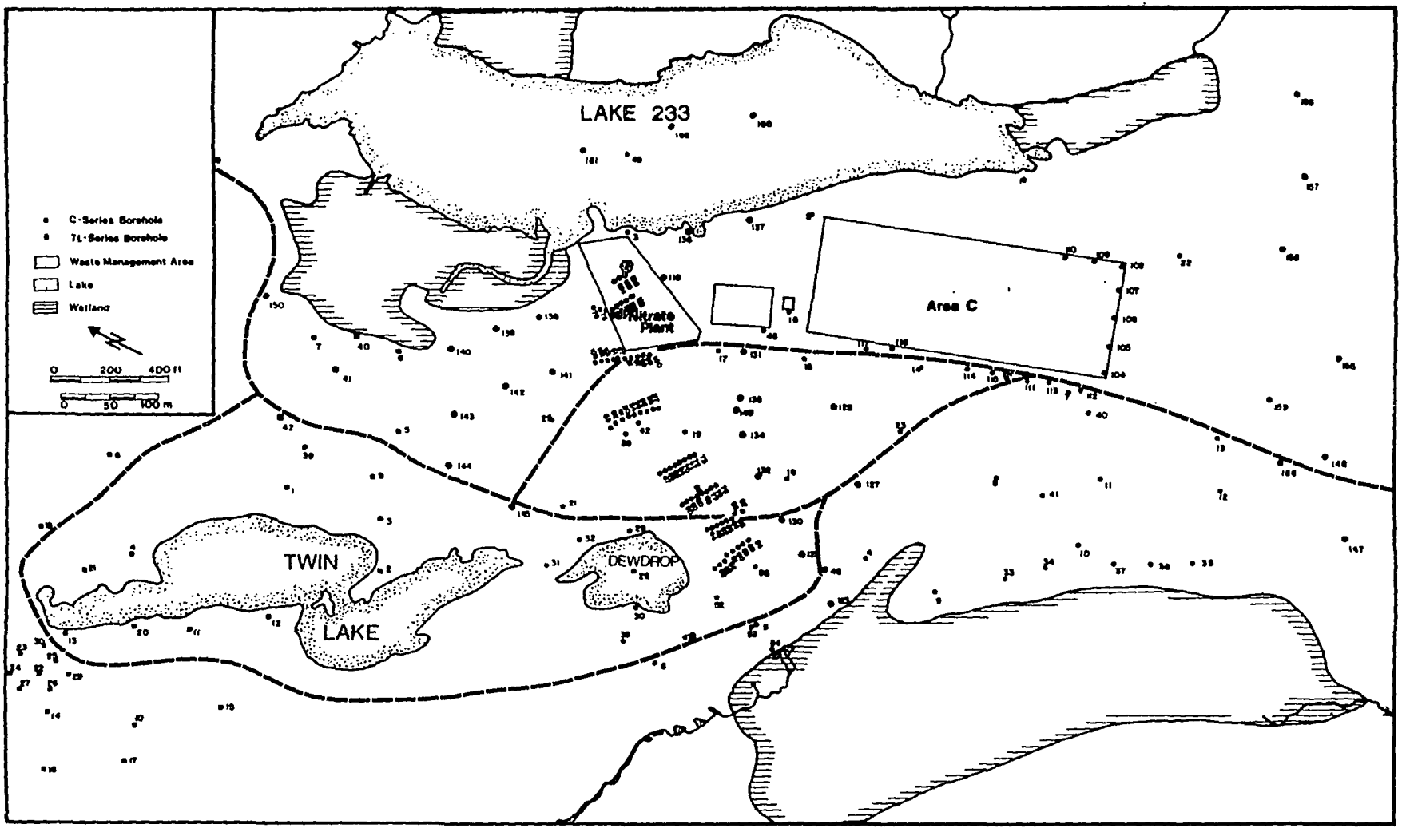

Figure 1b Plan-view of the study area and monitoring network

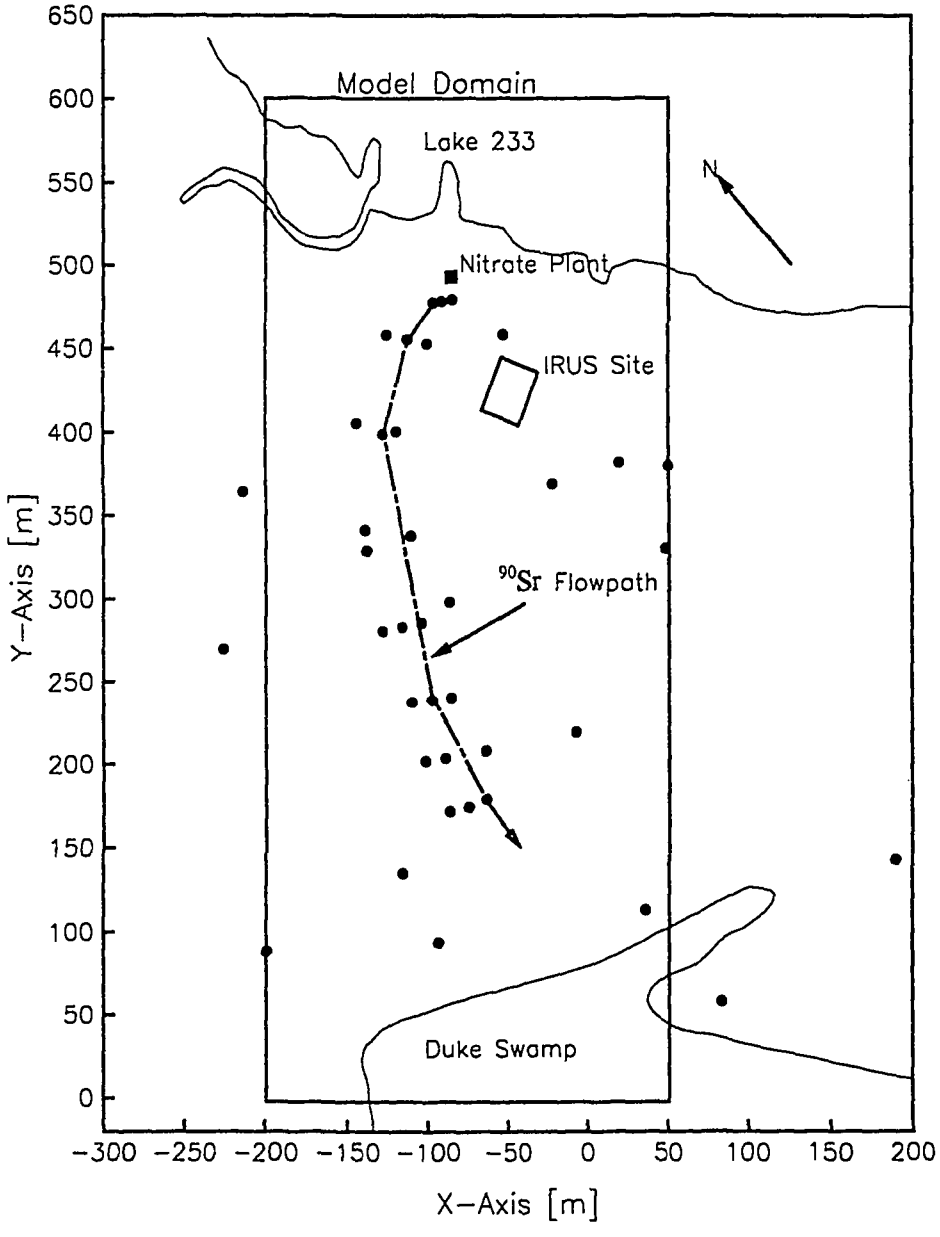

Figure 2 Model domain, ^{90}Sr flowpath and IRUS Site

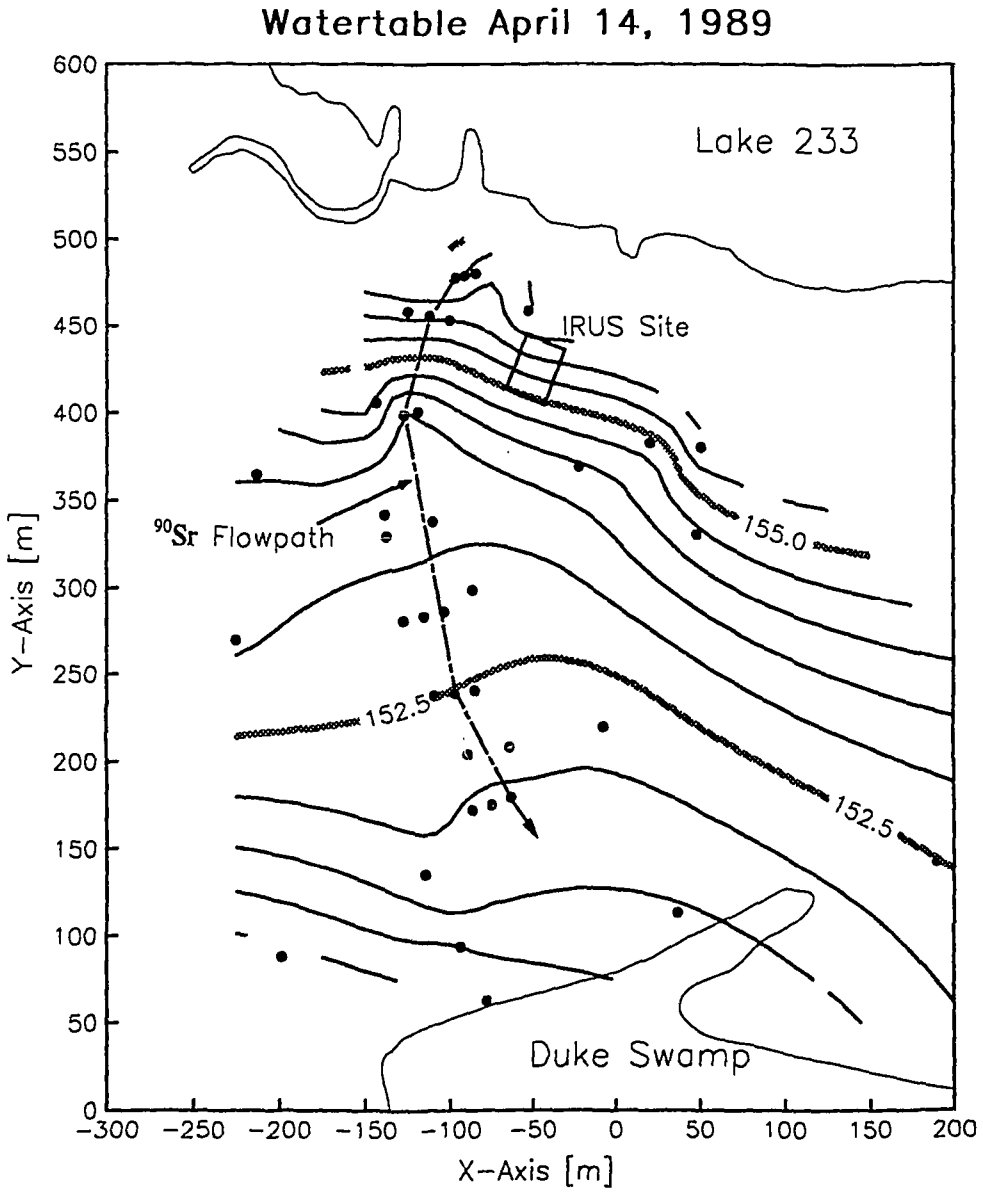

Figure 3a Measured watertable elevation [masl], April 14, 1989

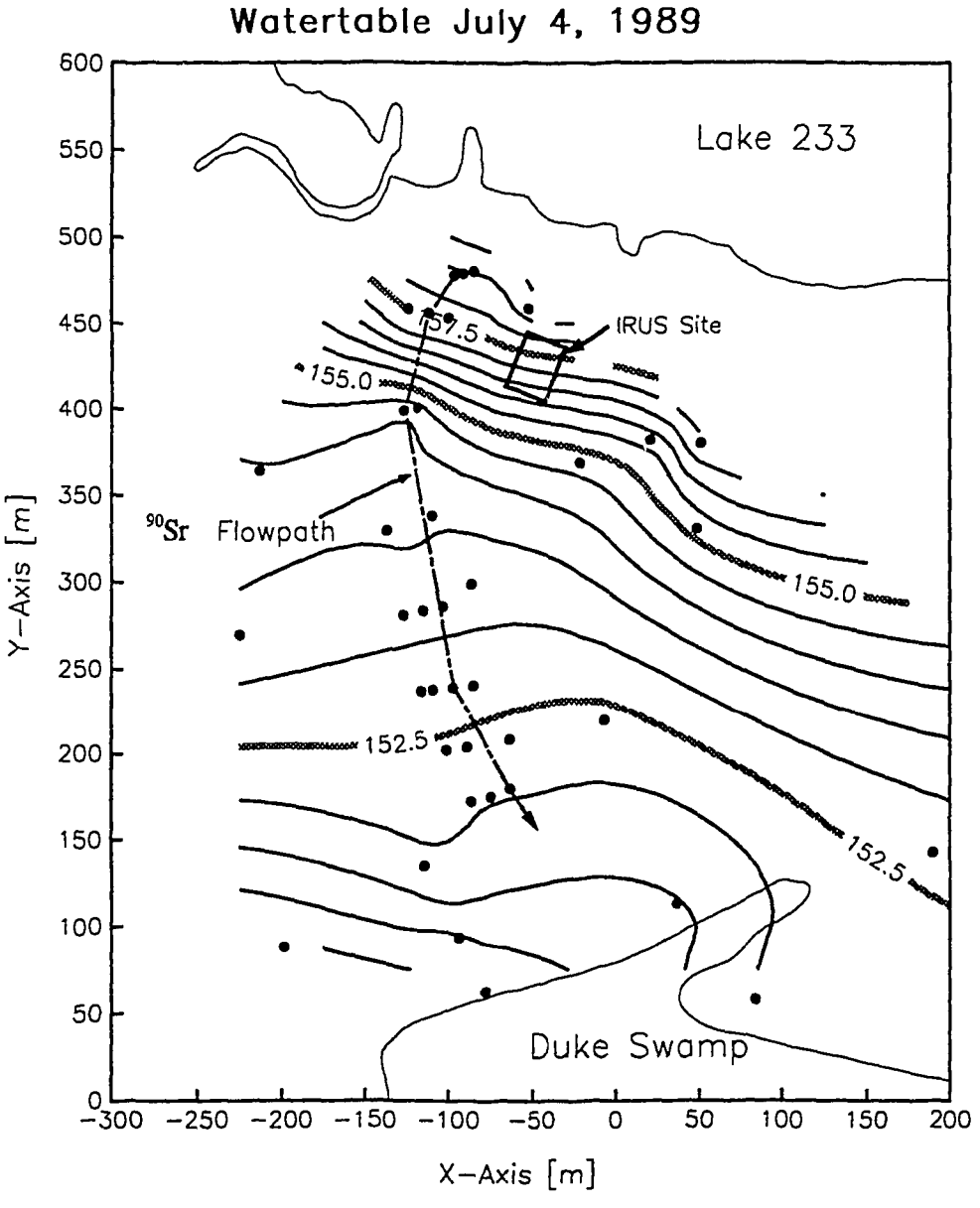

Figure 3b Measured watertable elevation [masl], July 4, 1989

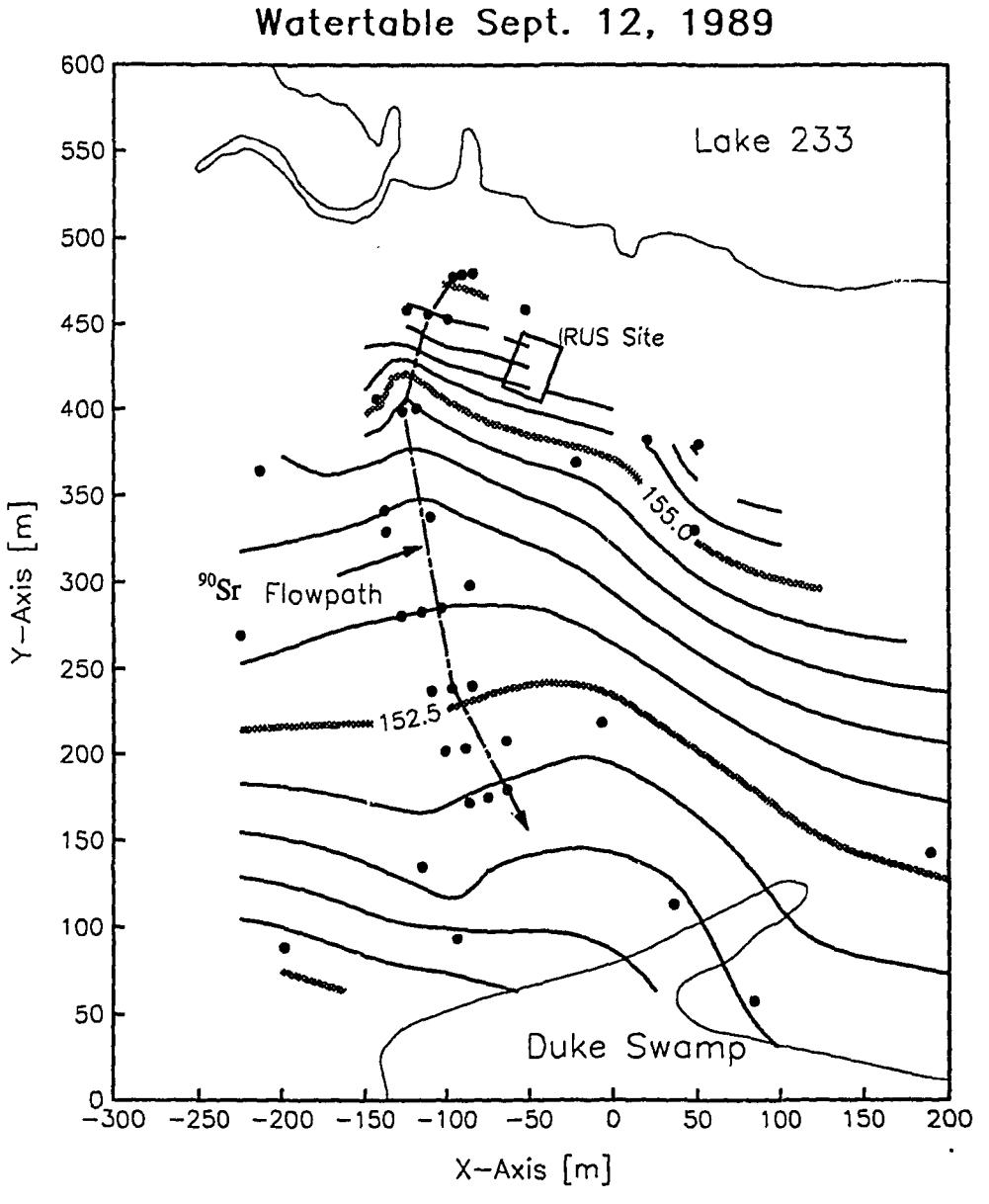

Figure 3c Measured watertable elevation [masl], September 12, 1989

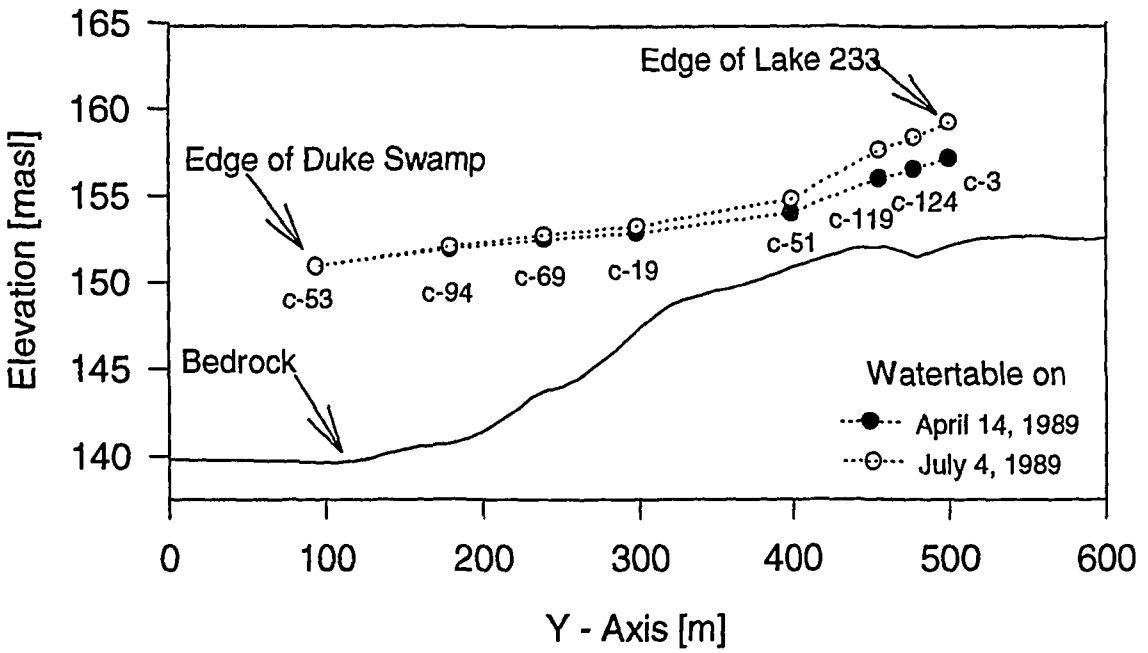

Figure 4 Increase in watertable elevation along the ^{90}Sr flow path over spring recharge

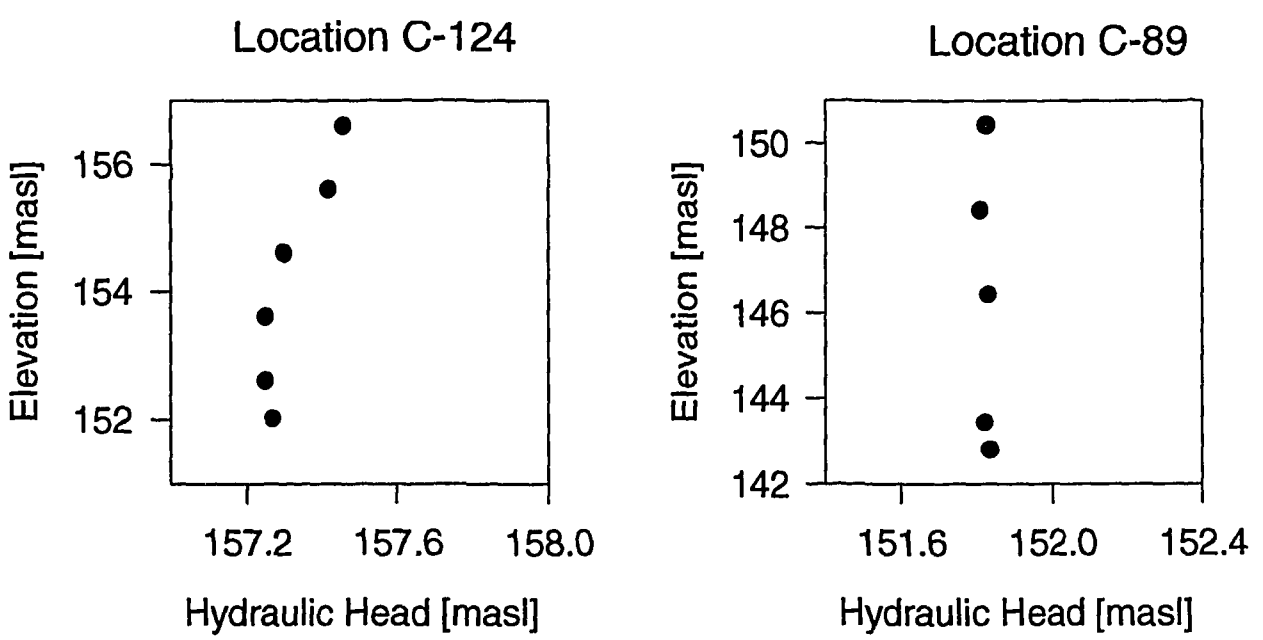

Figure 5 Hydraulic head depth profiles at monitoring wells C-124 and C-89 located 50 m and 375 m downstream of Lake 233

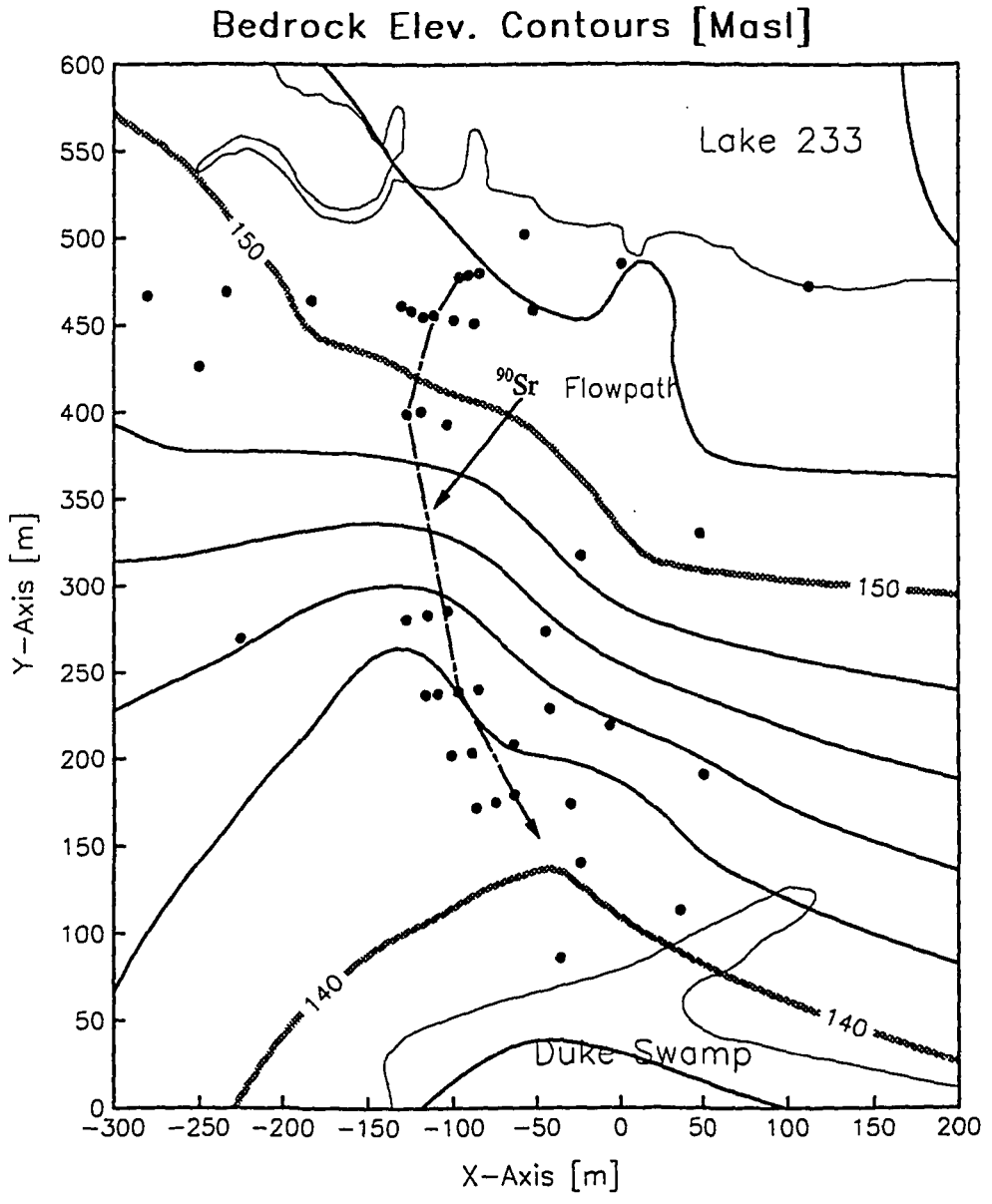

Figure 6 Bedrock elevation topography [masl]

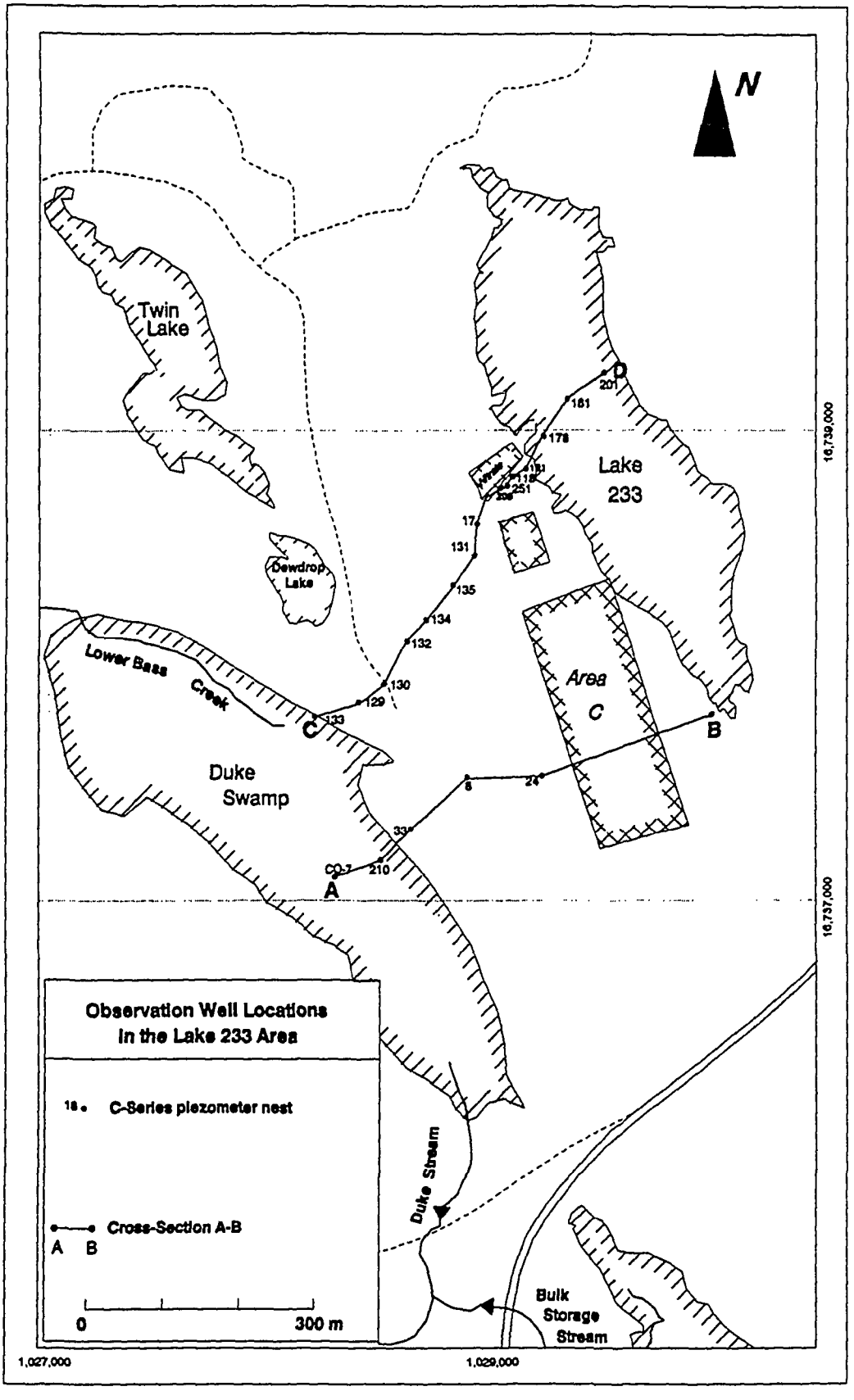

Figure 7 Plan-view showing locations of stratigraphic cross-sections A-B and C-D

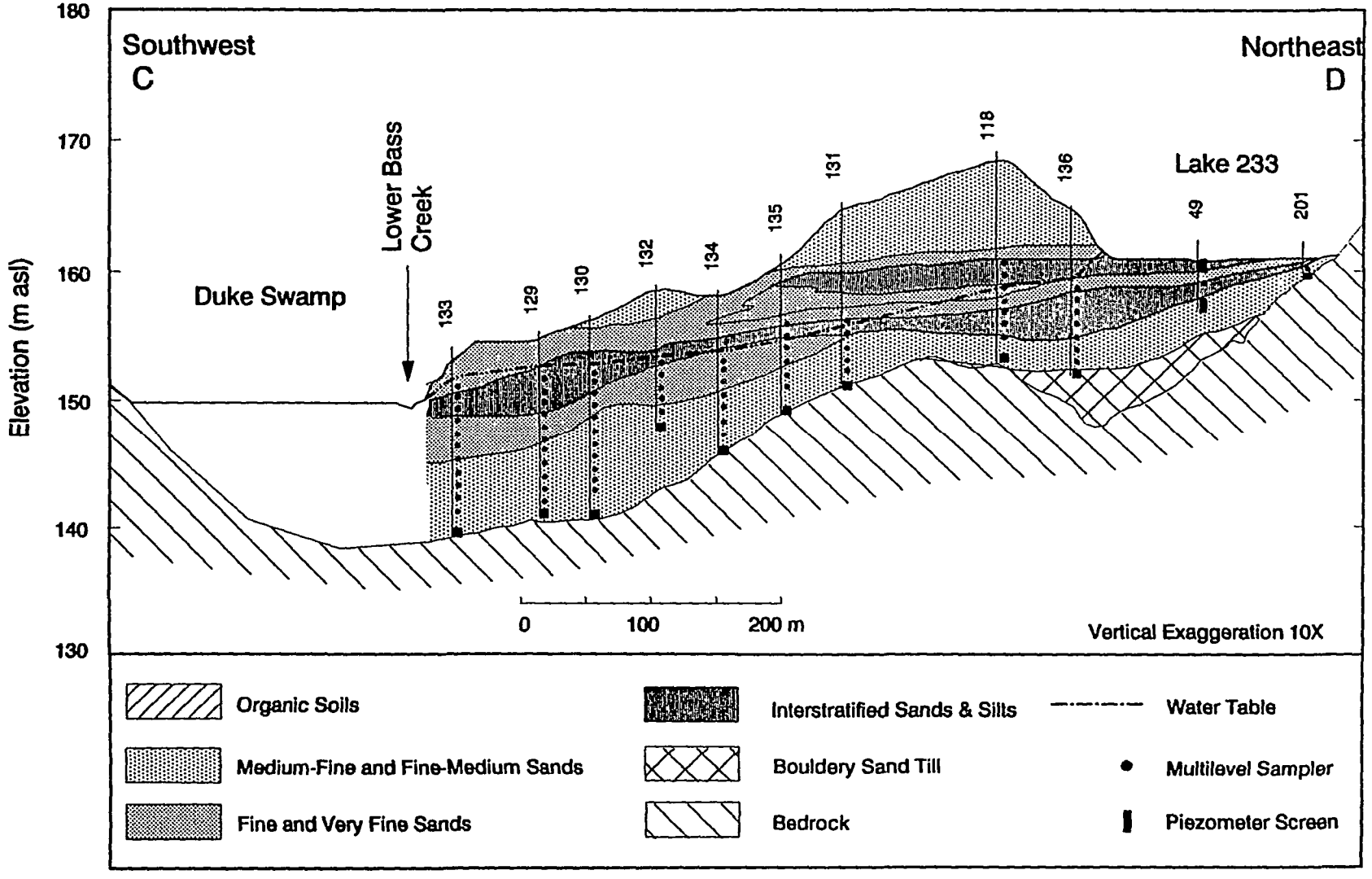

Figure 8 Stratigraphic cross-section along line C-D

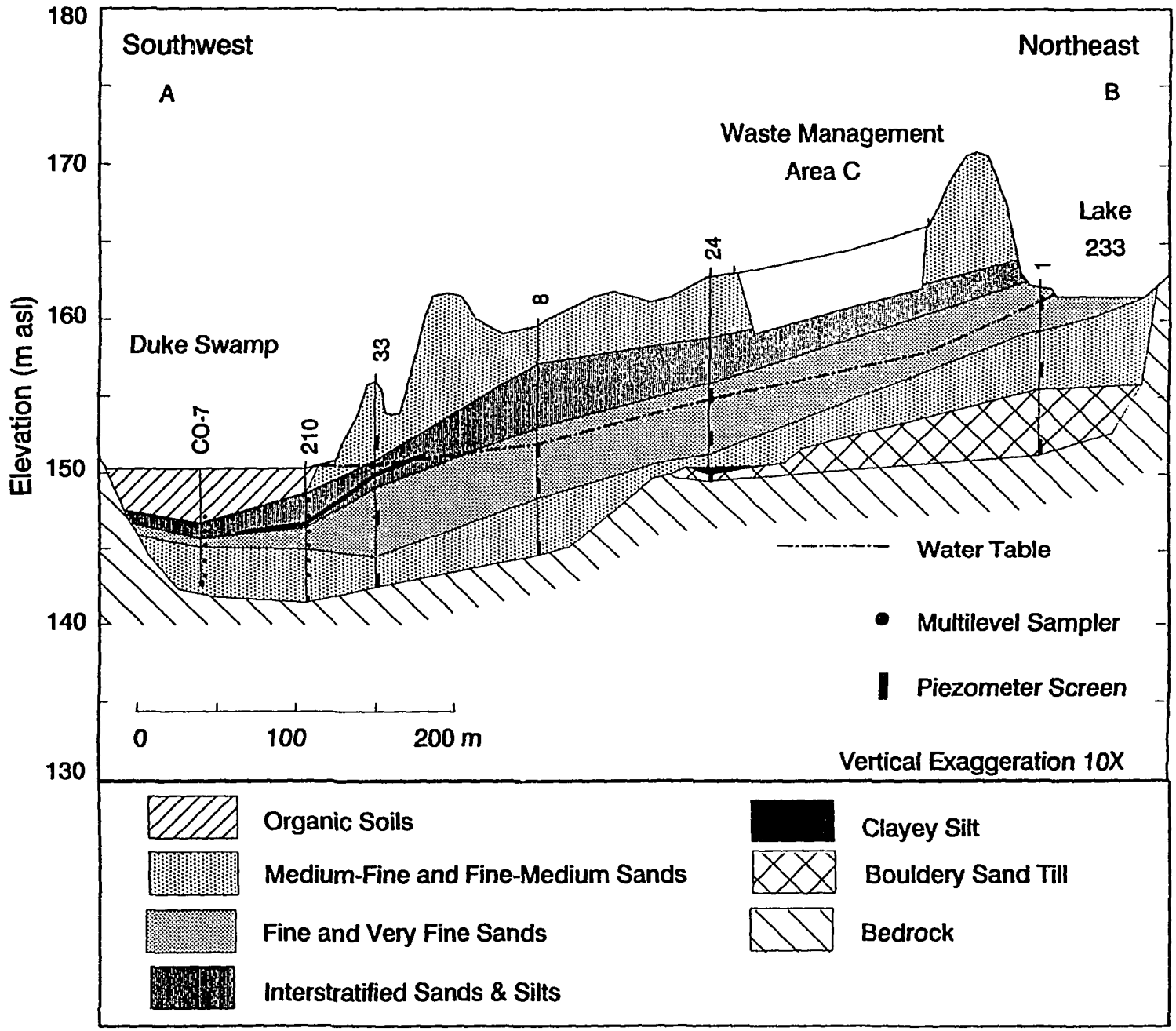

Figure 9 Stratigraphic cross-section along line A-B

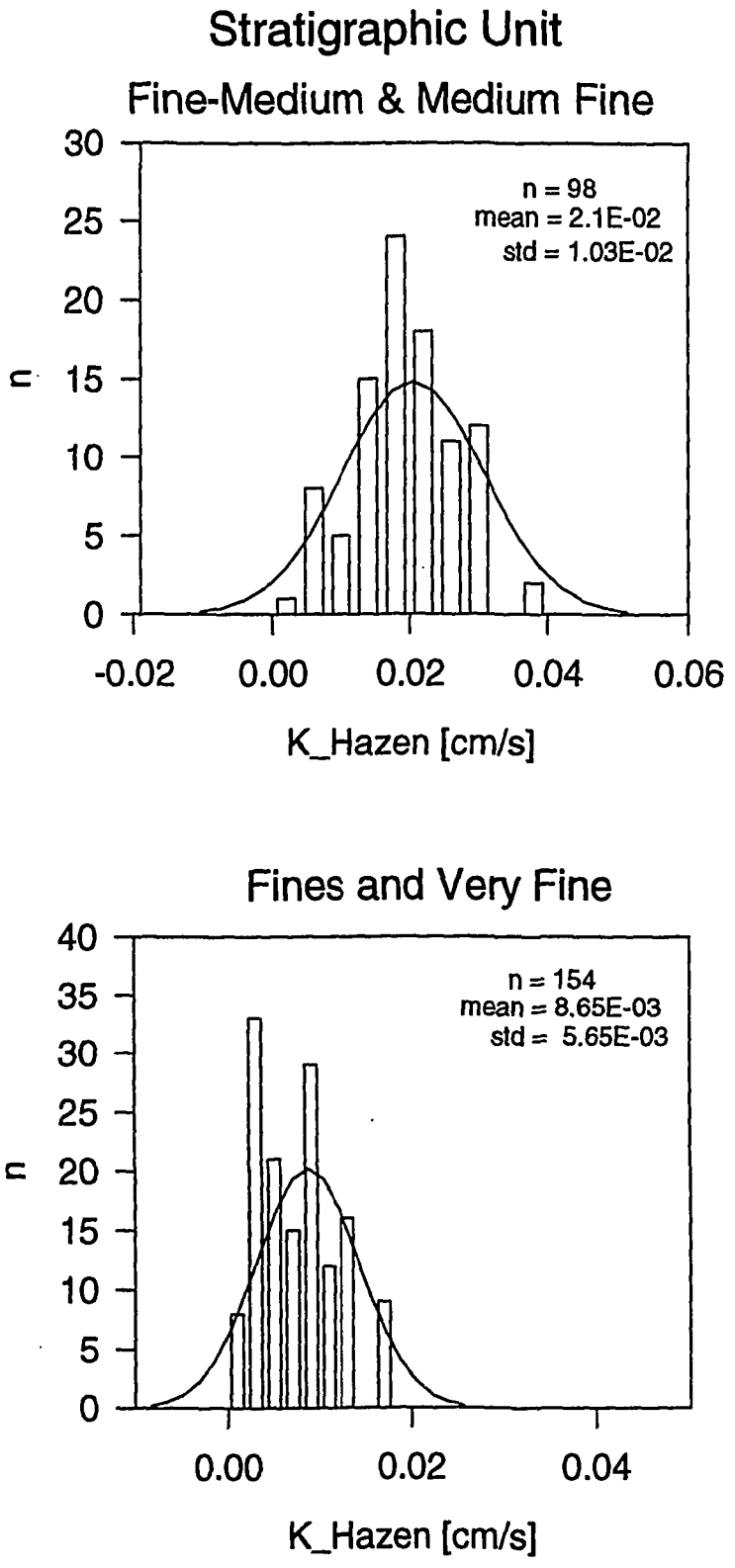

Figure 10 Histograms of Hazen-derived hydraulic conductivities for the fine-medium & medium-fine stratigraphic unit (top), and the fines & very fine stratigraphic unit (bottom)

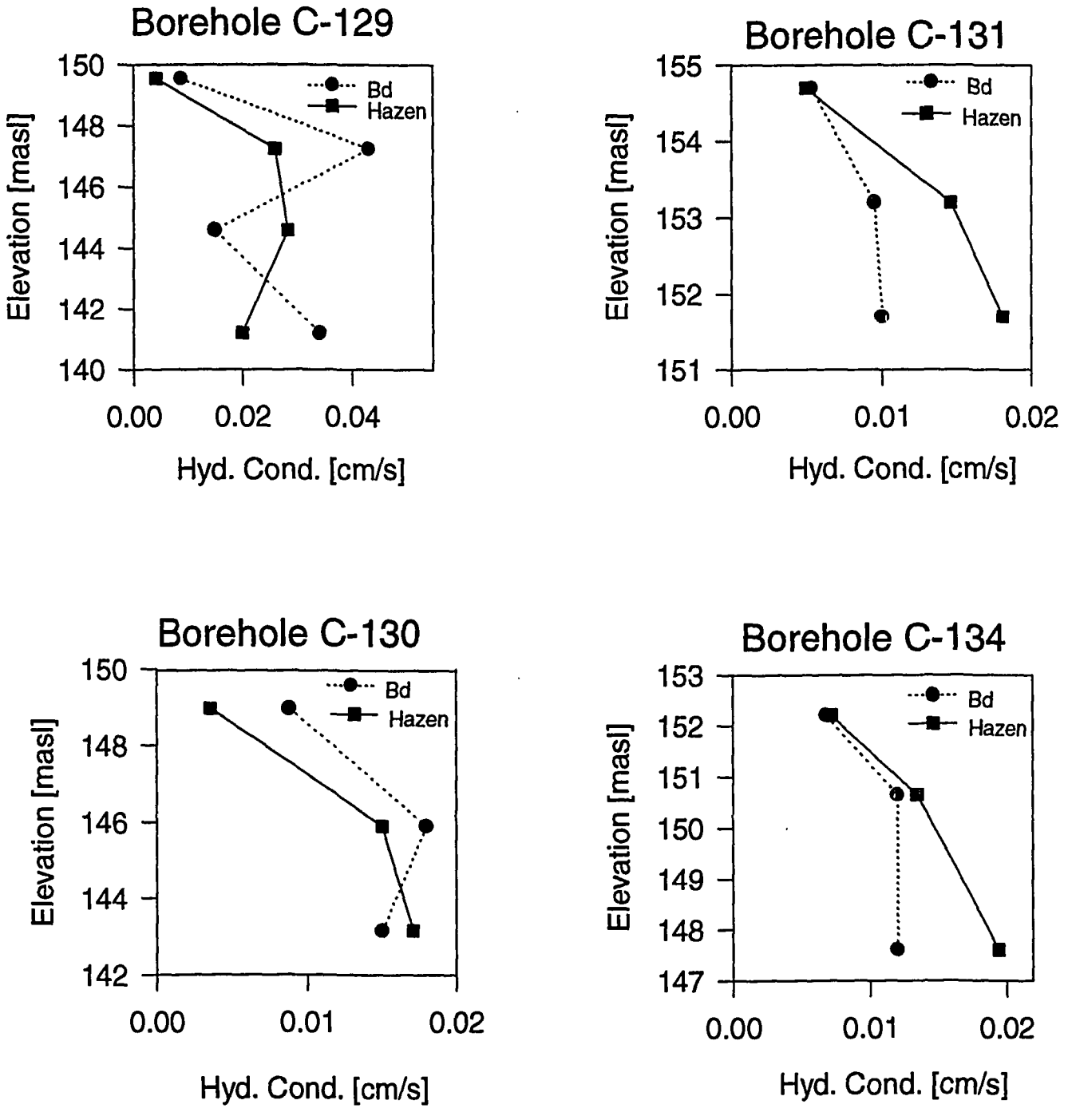

Figure 11 Hazen-derived and borehole dilution velocity derived hydraulic conductivity profiles. Hazen - Solid line with marker, Borehole dilution - dotted line with marker

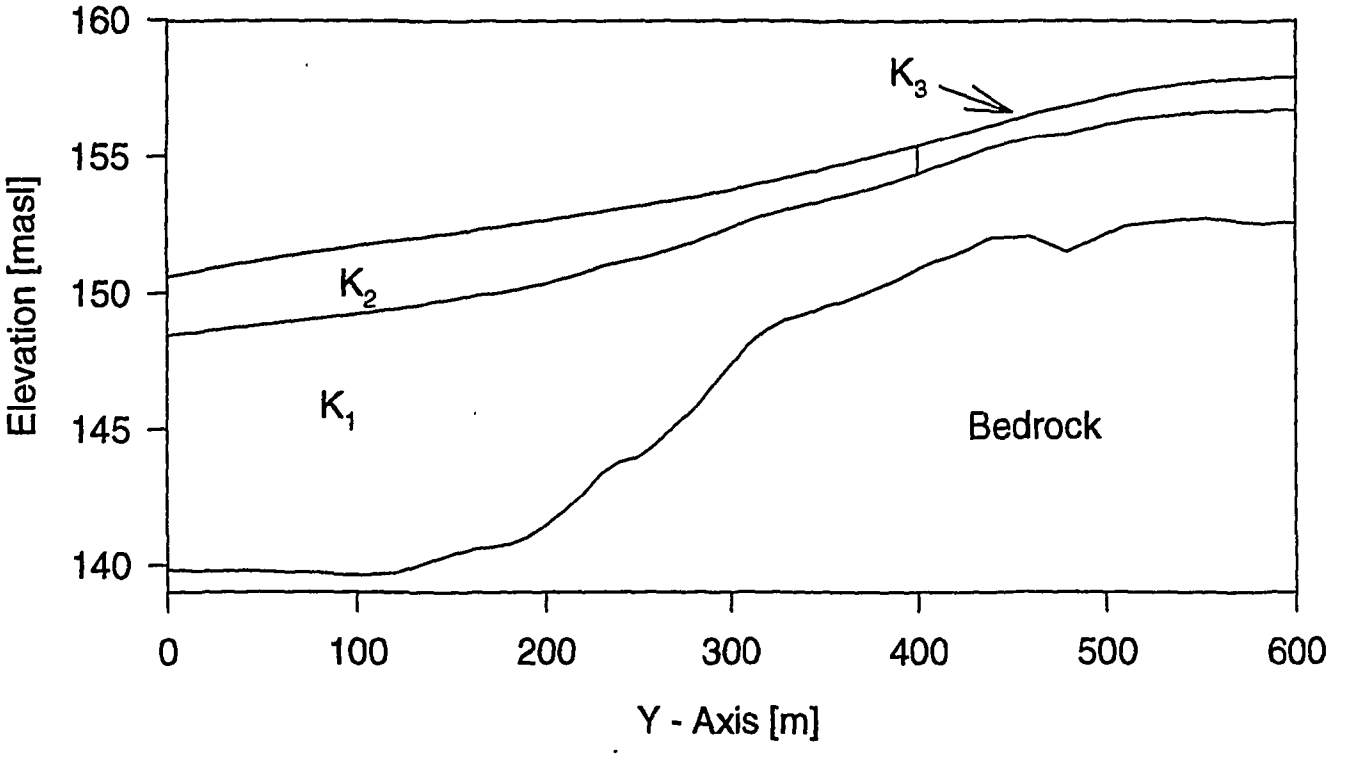

Figure 12 Cross-section of the hydraulic conductivity distribution for flow modelling along the longitudinal axis of the model domain. K_1 - sandy unit, K_2 and K_3 - interstratified sands and silts

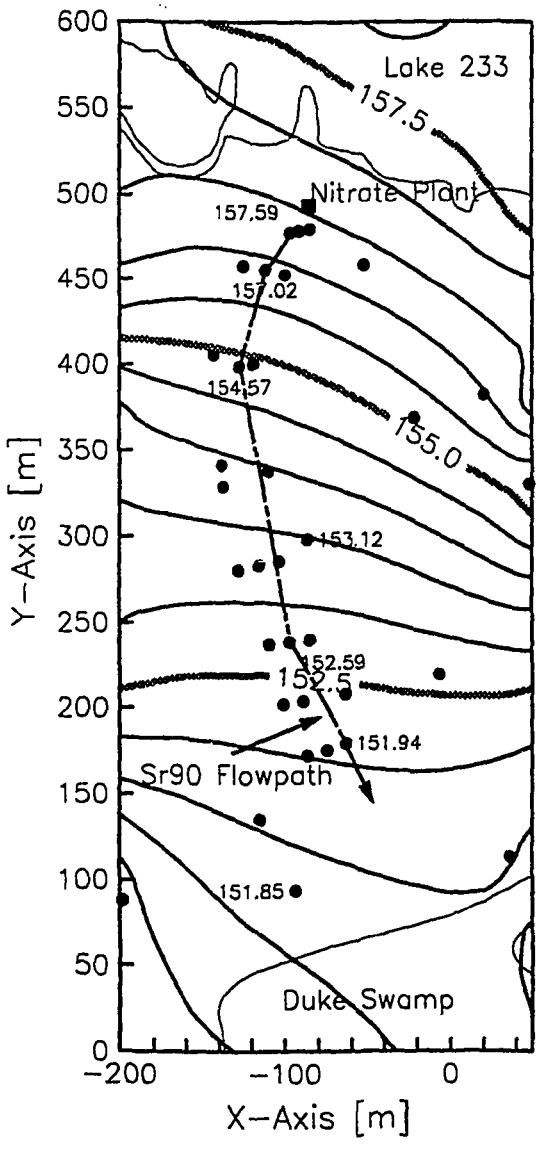

Figure 13 Simulated watertable contours, uncalibrated flow model. Observed September 12, 1989 watertable elevations are given at selected monitoring wells along the ^{90}Sr flowpath

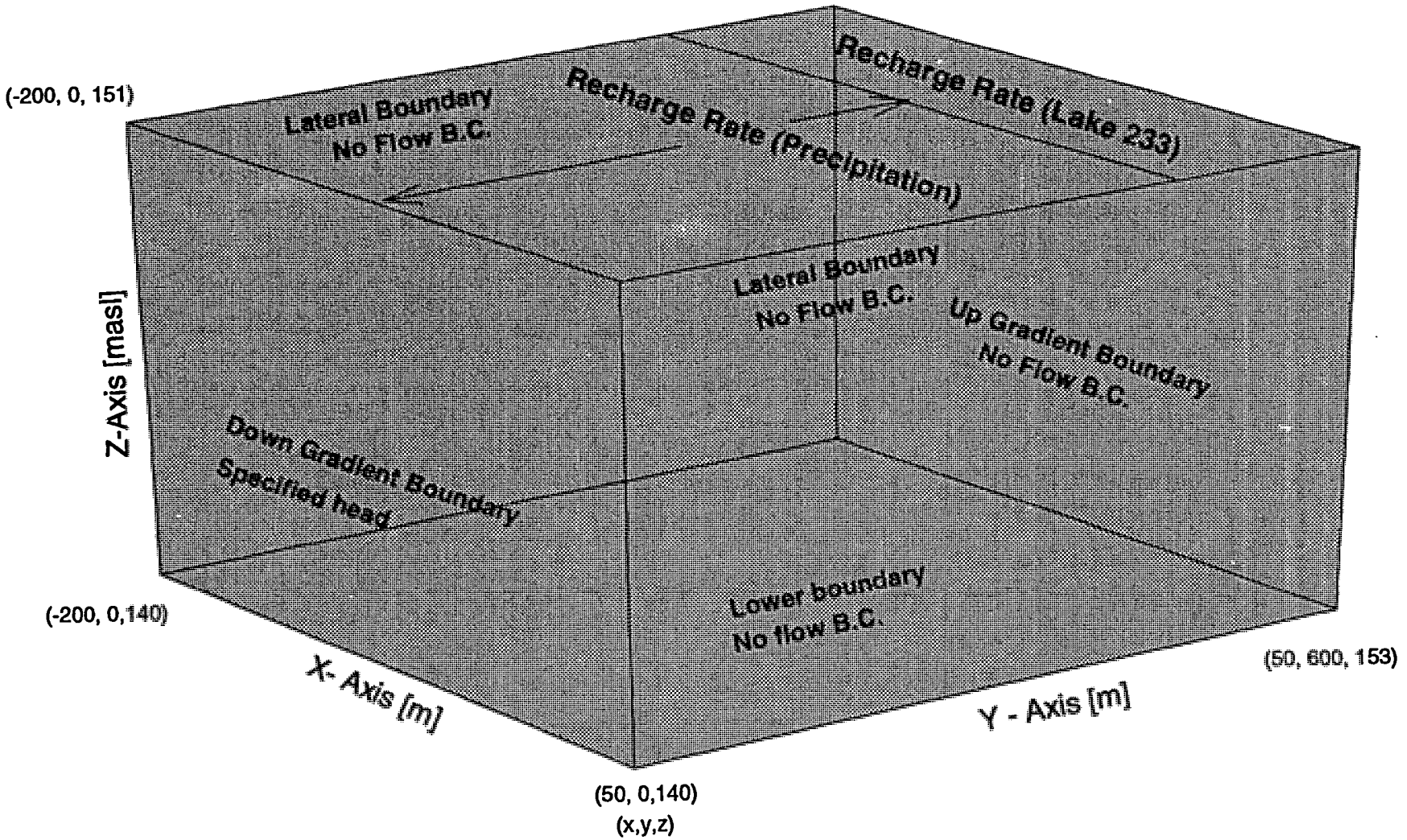

Figure 14 Schematic of model domain, boundary conditions and recharge for the calibrated model

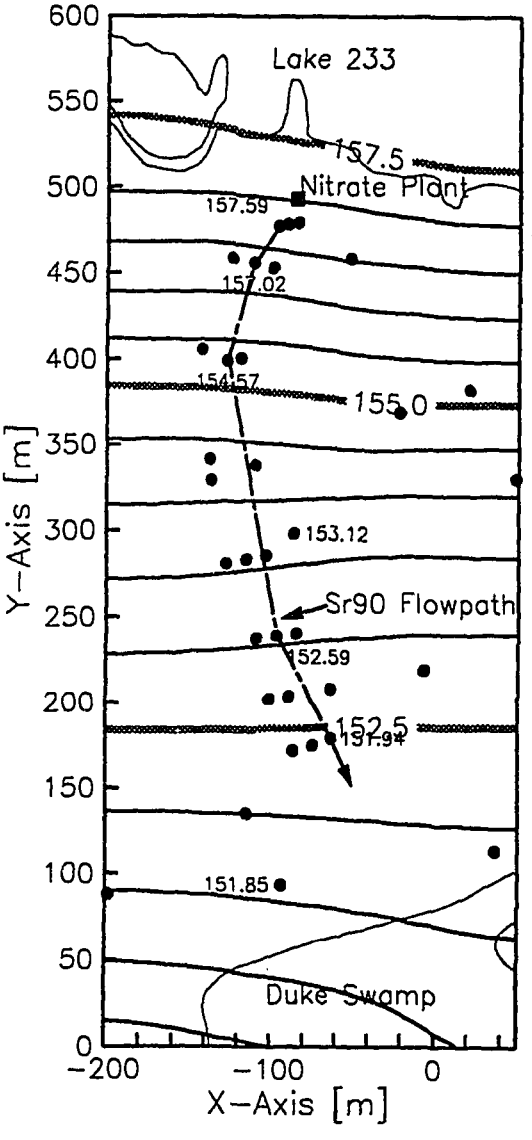

Figure 15 Simulated watertable contours, calibrated flow model incorporating recharge and the September 12, 1989 measured waterlevels along the ^{90}Sr flowpath

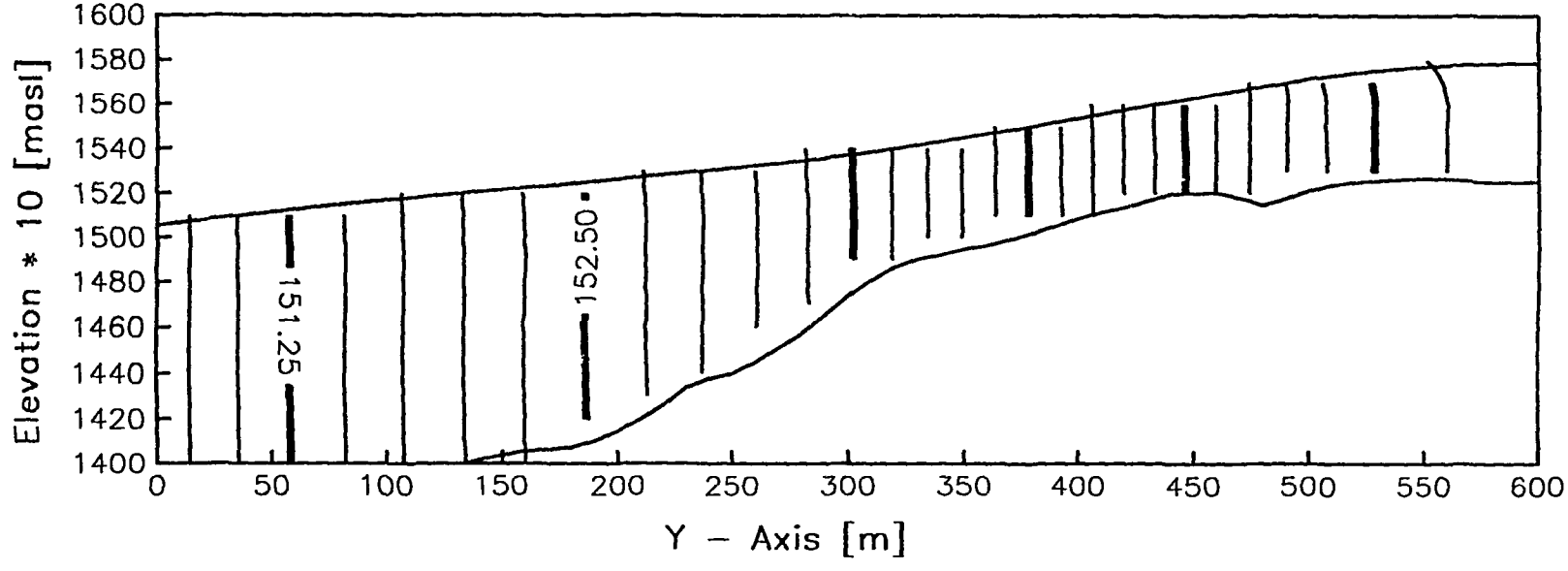

Figure 16 Simulated family of equipotentials in the vertical plane along the longitudinal-axis of the model domain

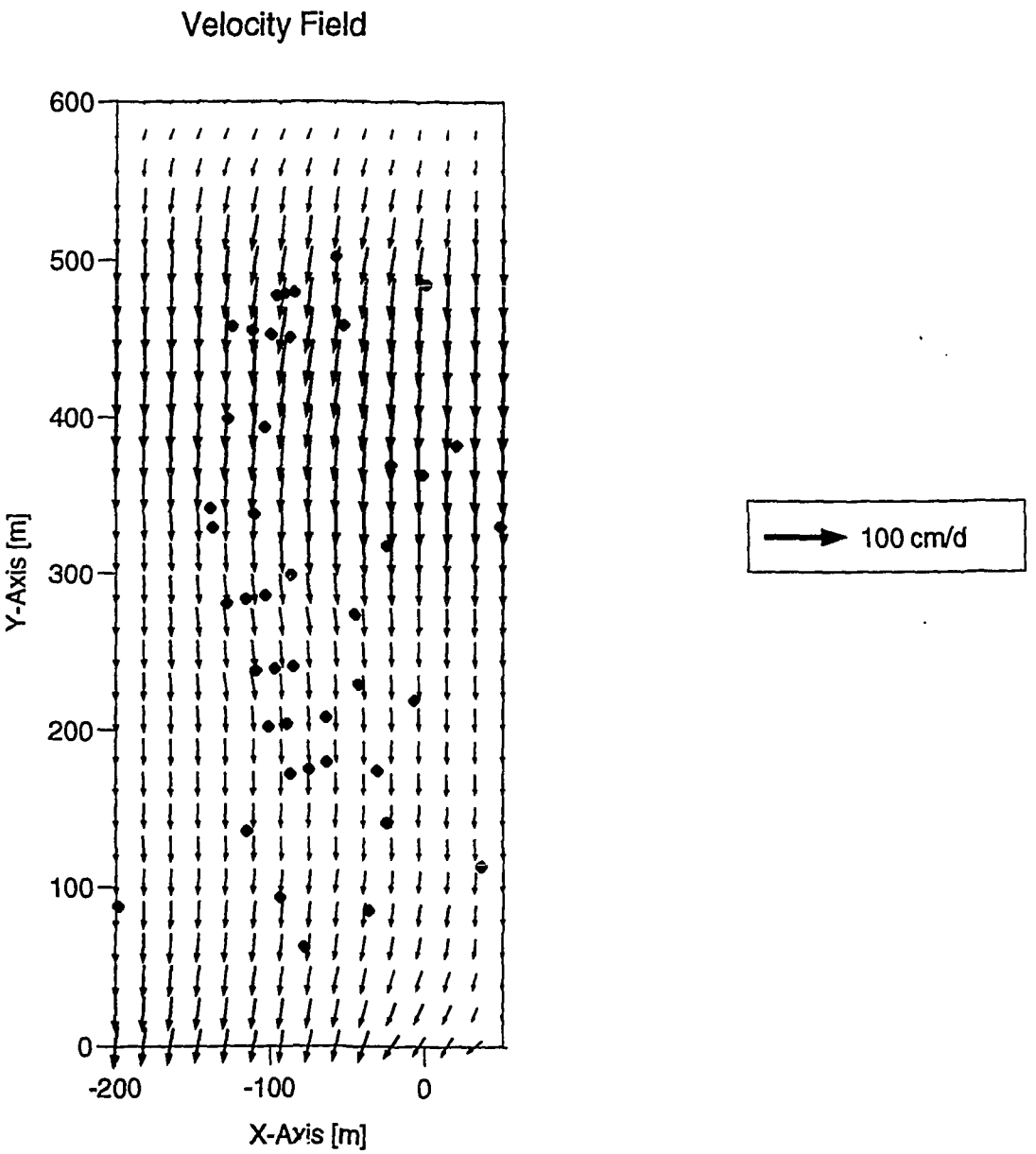

Figure 17 Projection of simulated velocity vectors in the plan-view

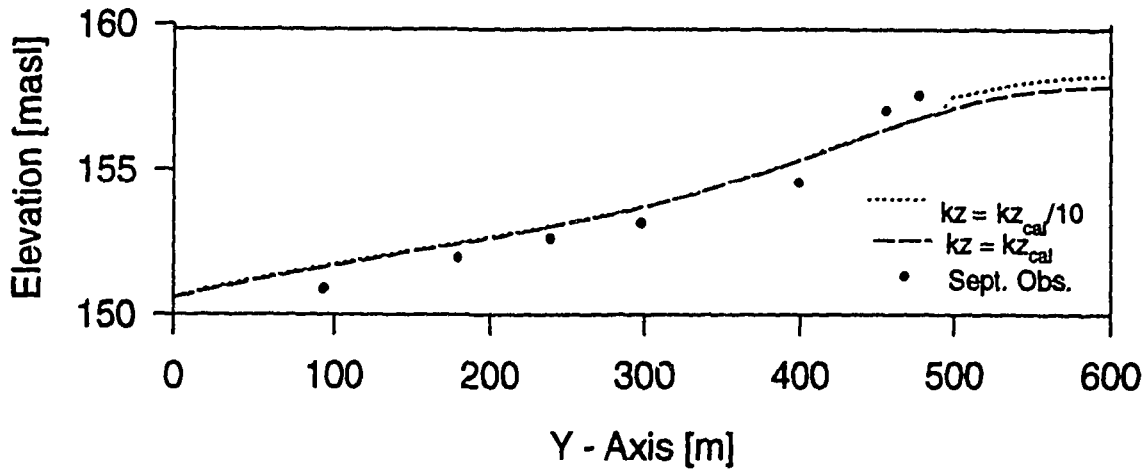

Figure 18 Sensitivity of the simulated watertable to the vertical conductivity of the interstratified sands and silts and the September 12, 1989 observed waterlevels

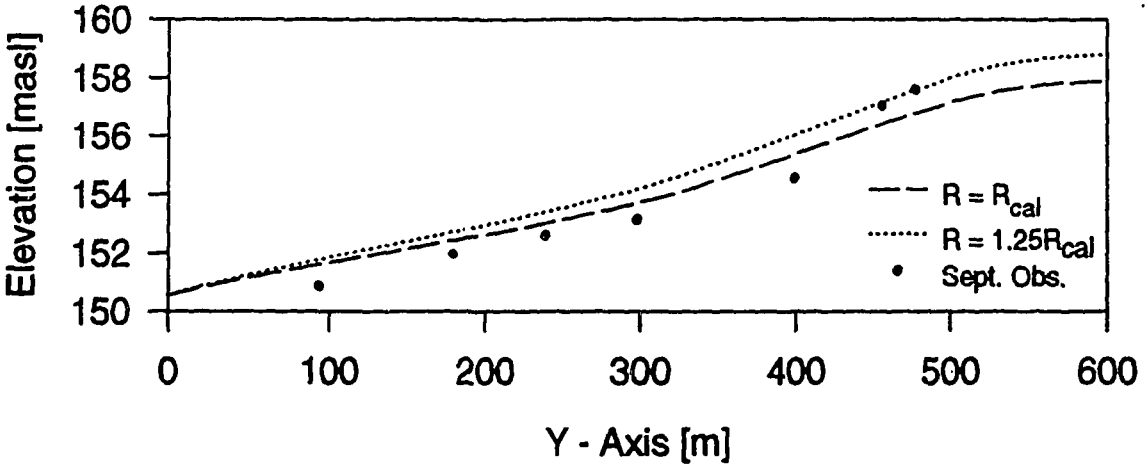

Figure 19 Sensitivity of the simulated watertable to a 25% increase in Lake 233 recharge

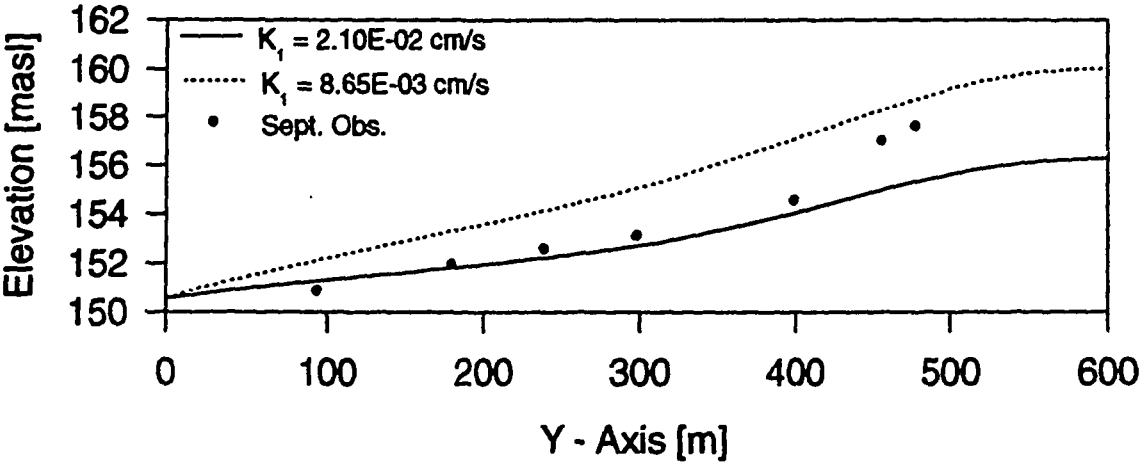

Figure 20 Sensitivity of the simulated watertable to the hydraulic conductivity of the sandy unit K_1

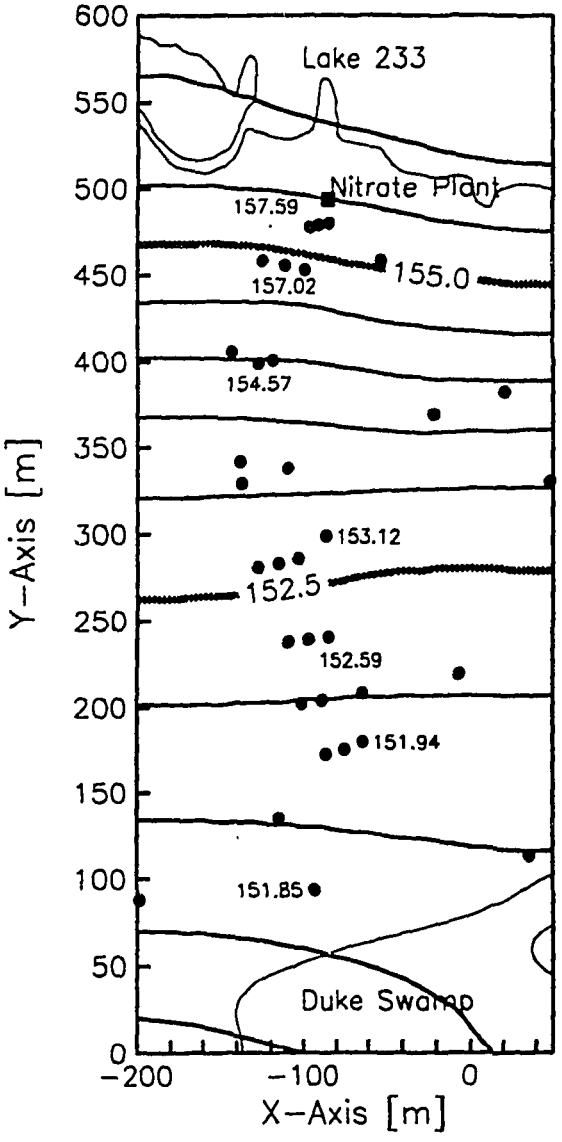

Figure 21 Simulated watertable contours for hydraulic conductivity of main sandy unit K_1, 8.65E-03 cm/s and September 12, 1989 measured waterlevels

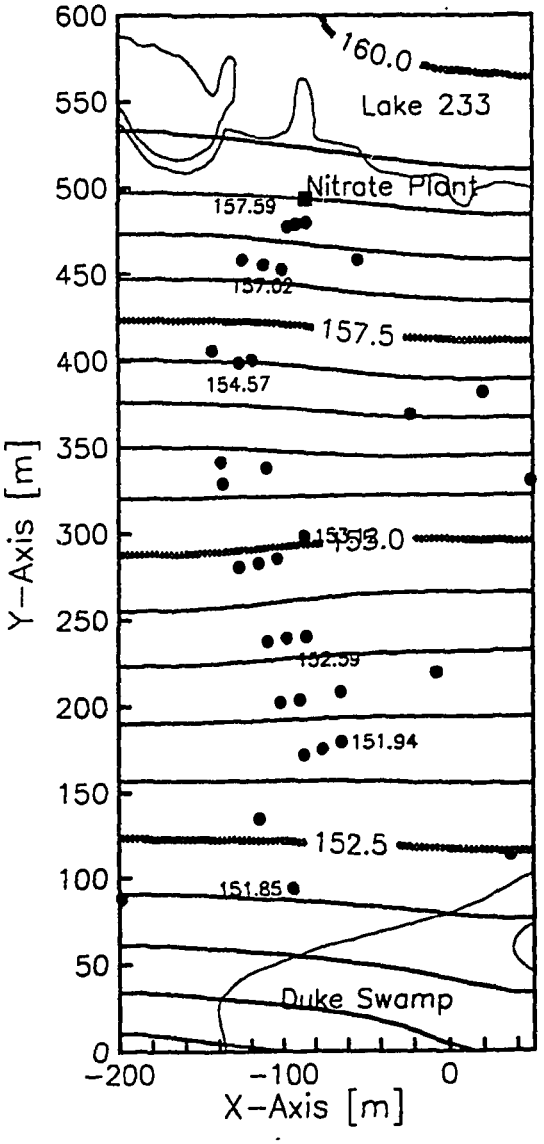

Figure 22 Simulated watertable contours for hydraulic conductivity of main sandy unit K_1, 2.1E-03 cm/s and September 12, 1989 measured waterlevels

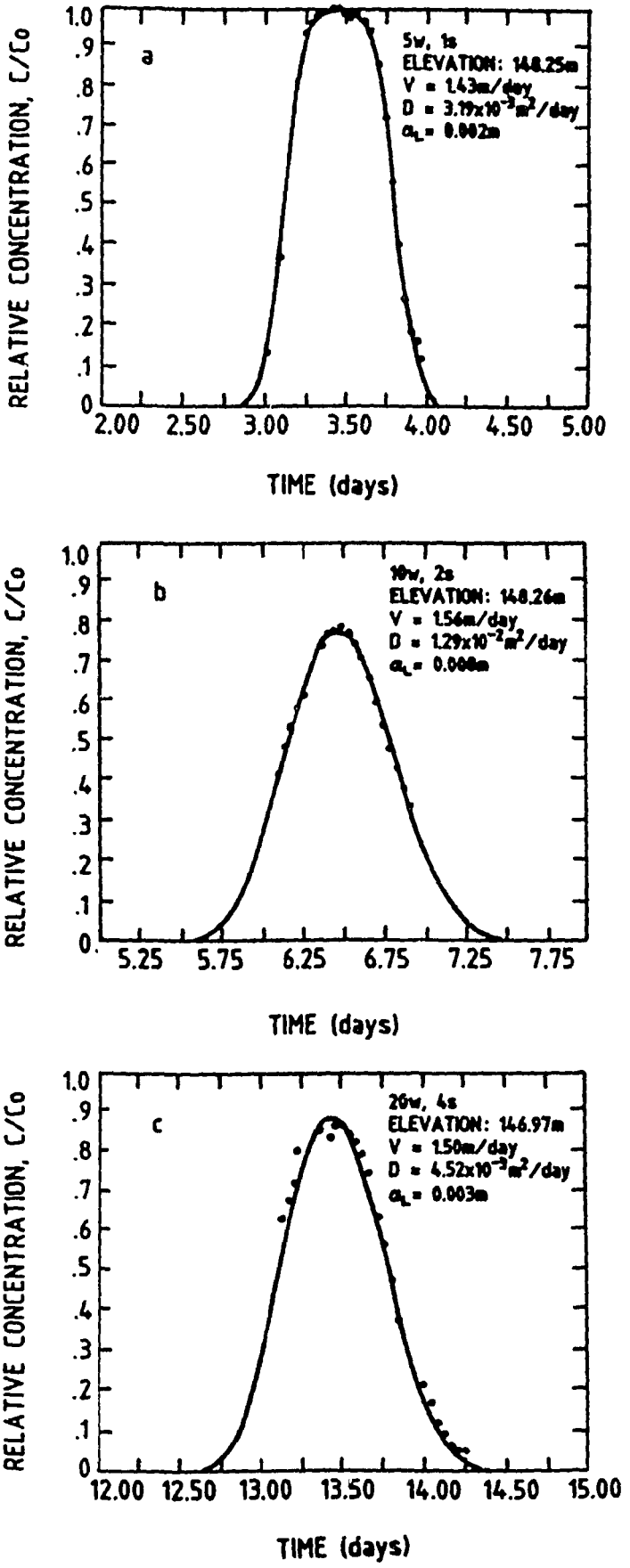

Figure 23 Local scale fitted breakthrough curves, 1983 Twin Lake tracer test at distances 5 m (top), 10 m (middle) and 20 m (bottom), from the injection well. Fitted - solid line, measured - marker

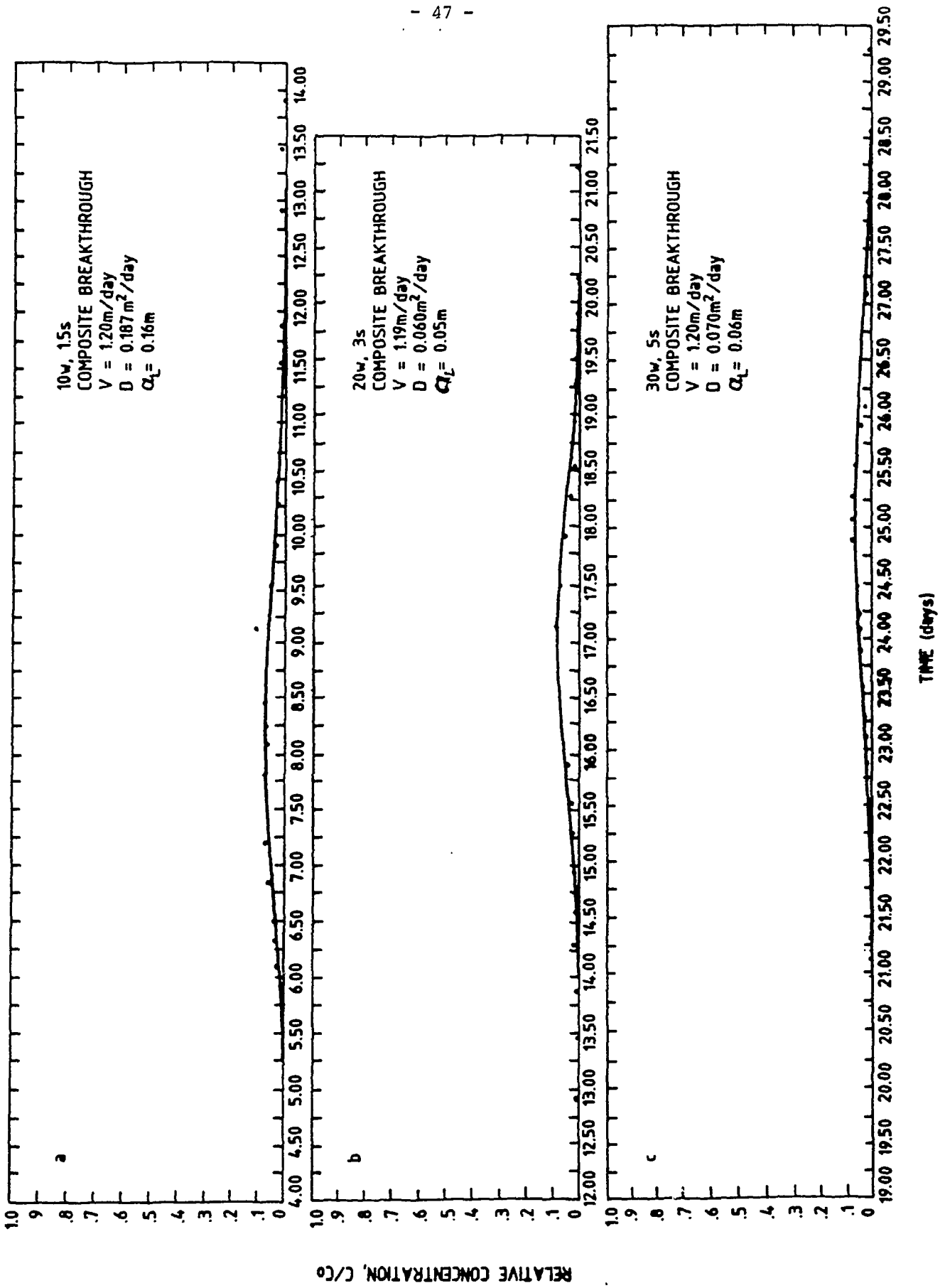

Figure 24 Plume scale fitted breakthrough curves at distances of 10 m (top), 20 m (middle) and 30 m (bottom) from the injection well. Fitted - solid line, measured - marker

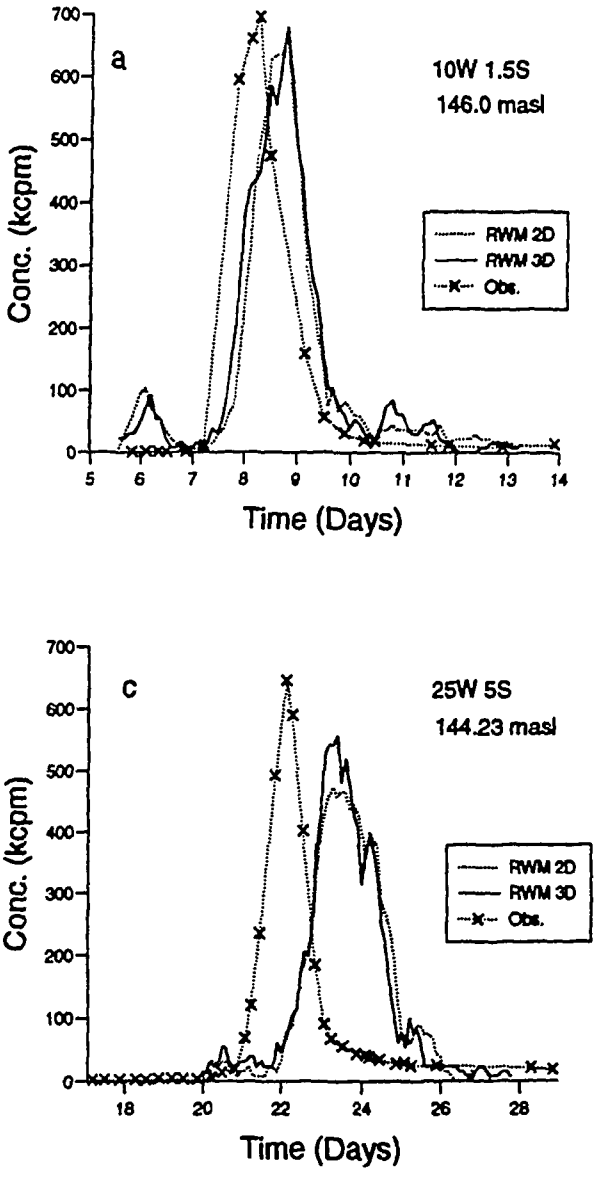

Figure 25 2-D and 3-D simulated and measured local scale breakthrough curves, 1983 Twin Lake tracer test for distances 10 m and 25 m from the injection well.

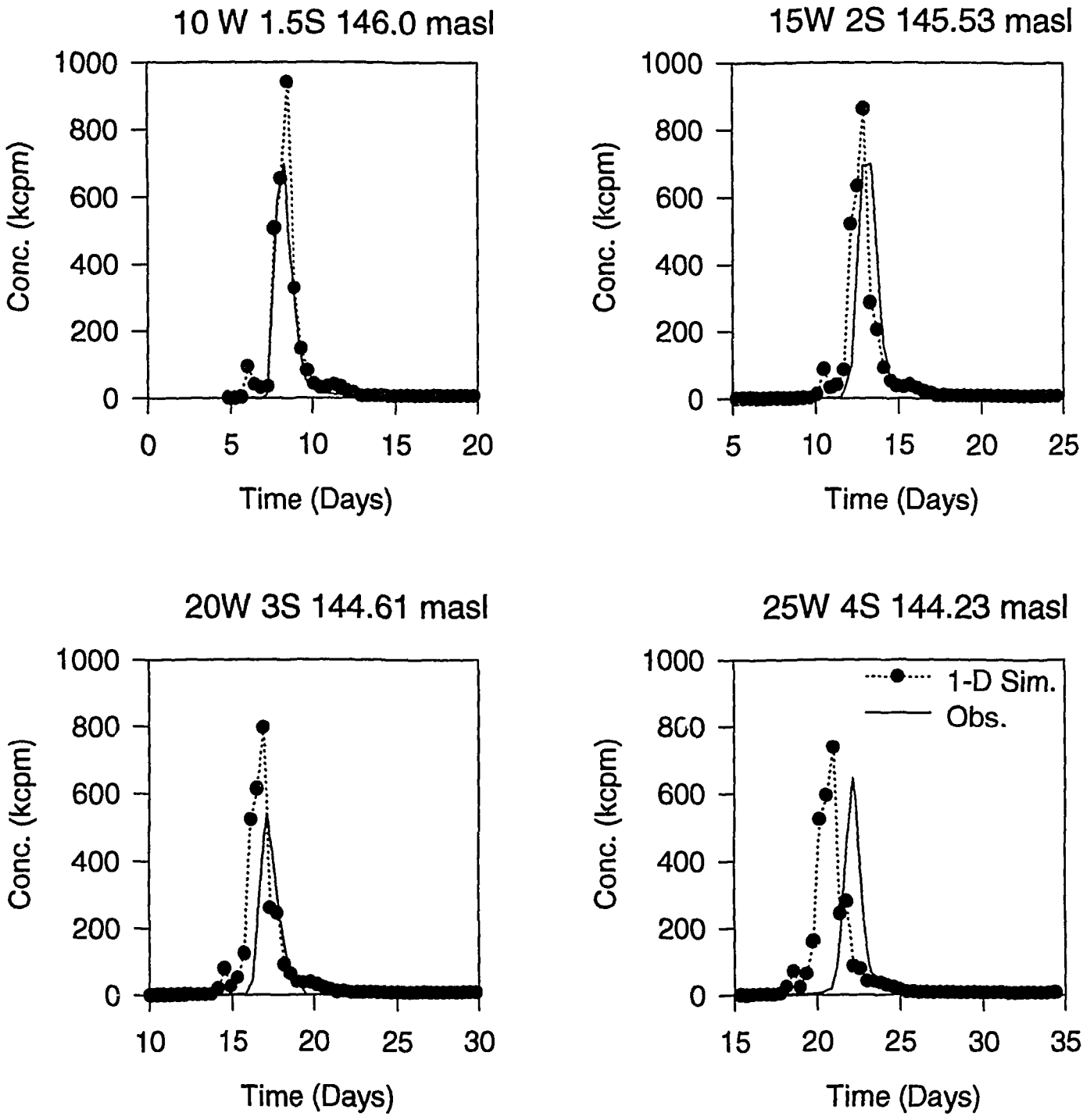

Figure 26 Simulated 1-D local scale breakthrough curves, 1983 tracer test, for locations 10, 15, 20, and 25 m from the injection well. Simulated - dotted line with marker, Measured - solid line

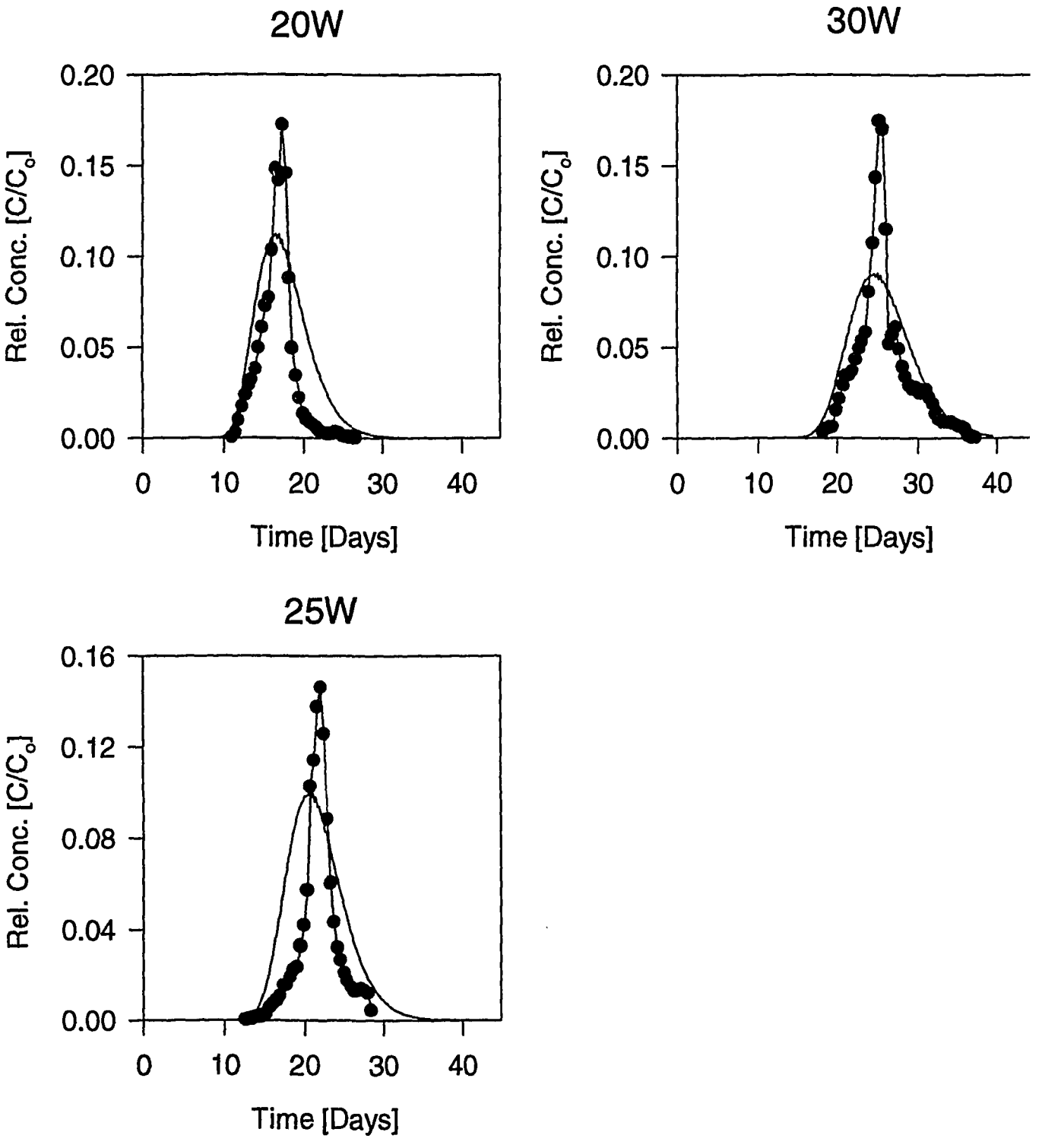

Figure 27 Simulated 1-D plume scale breakthrough curves, 1983 tracer test, for locations 20, 25 and 30 m from the injection well. Simulated - solid line, Measured - Solid line with markers

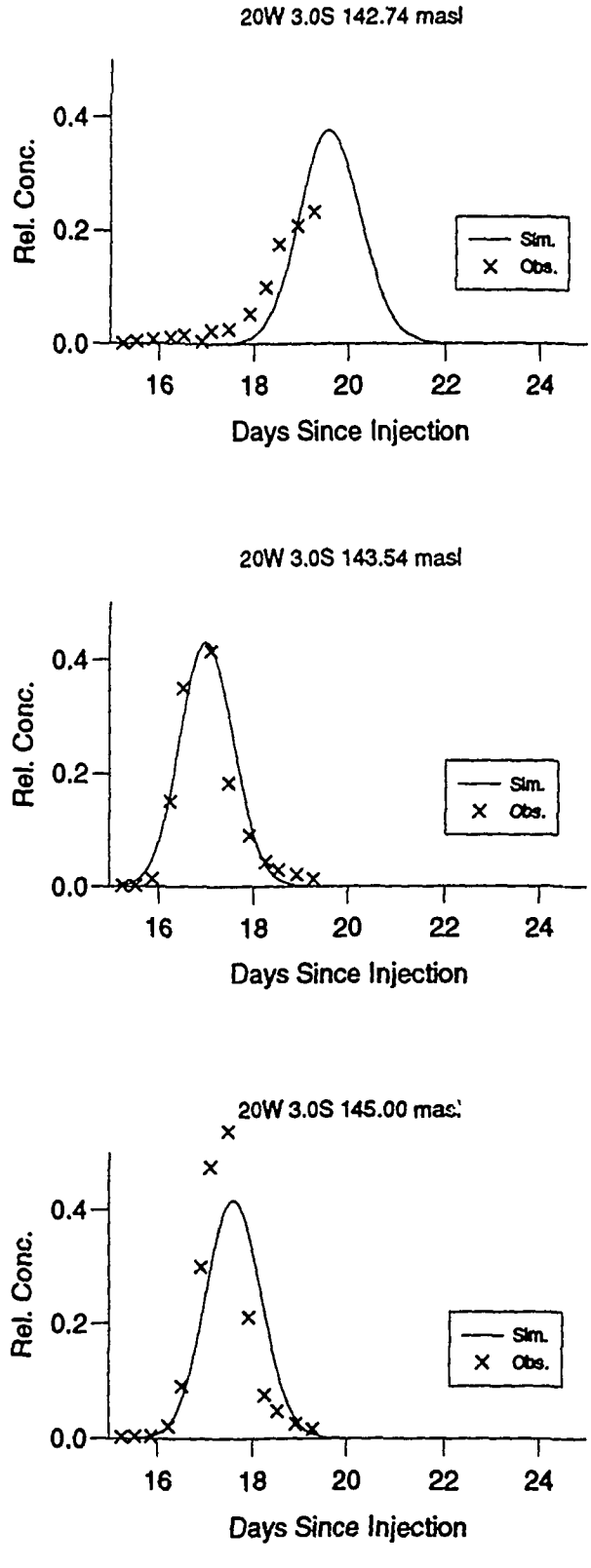

Figure 28 SYVAC-GEONET simulated local scale breakthrough curves, 1983 Twin Lake tracer test, for locations 20 m from injection well and elevations 142.74 masl (top), 143.54 masl (middle), and 145.0 masl (bottom). Simulated - Solid line, measured - marker.

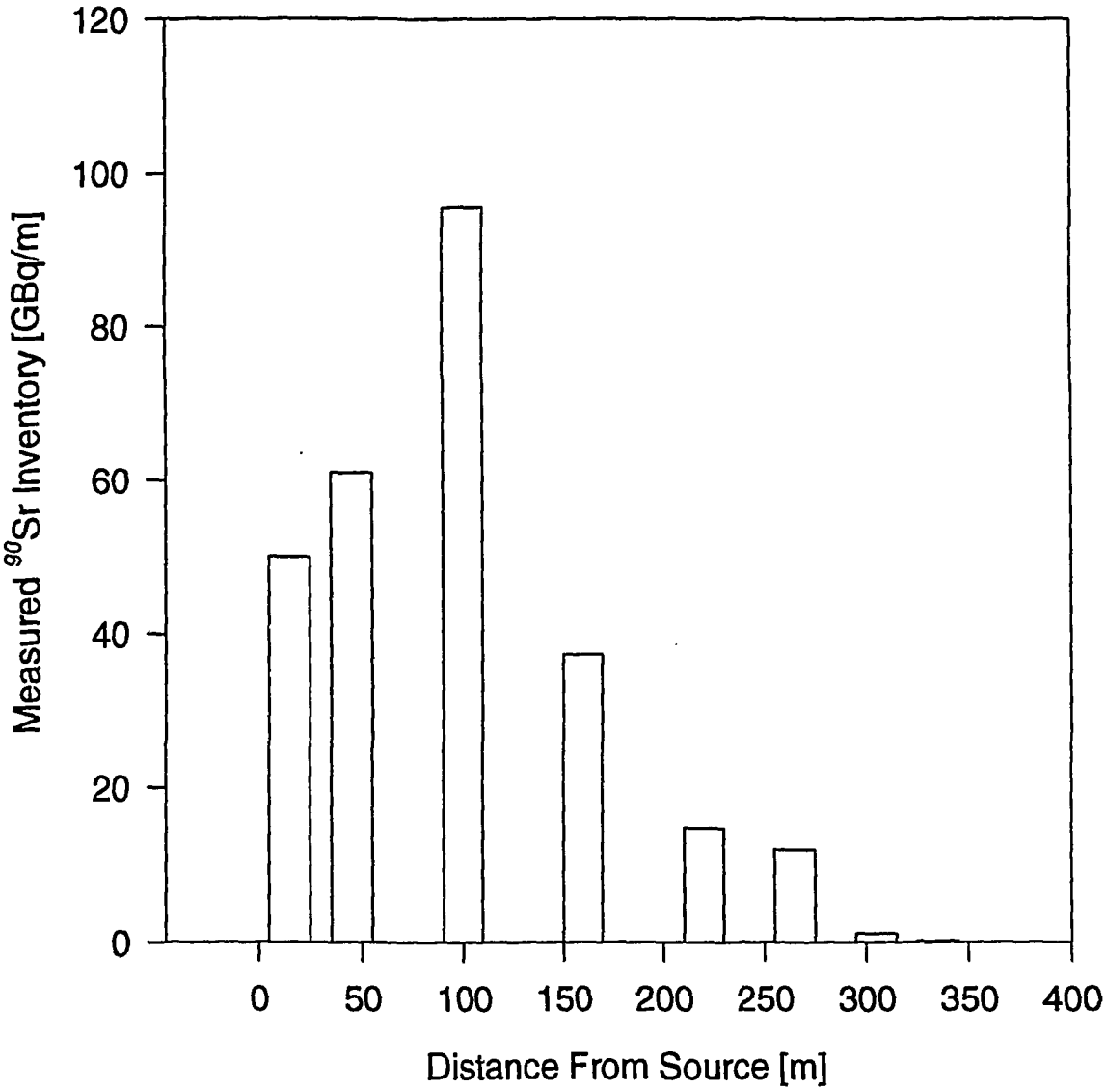

Figure 29 1983 ^{90}Sr distribution as a function of distance from the source

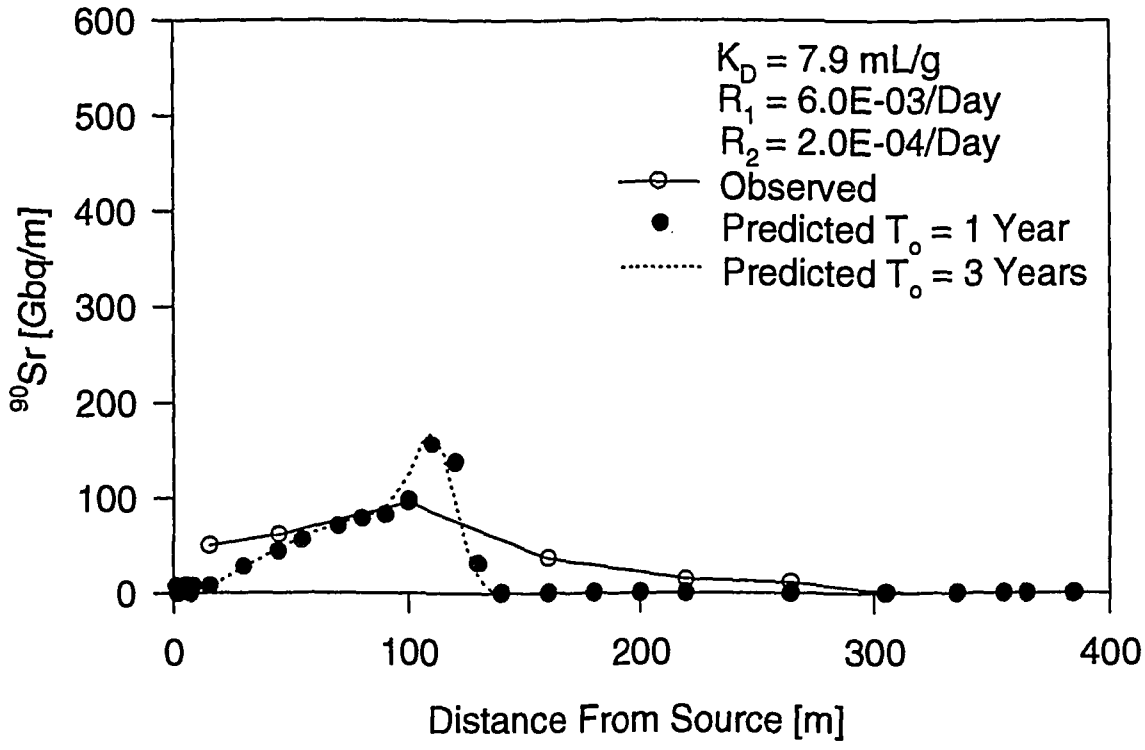

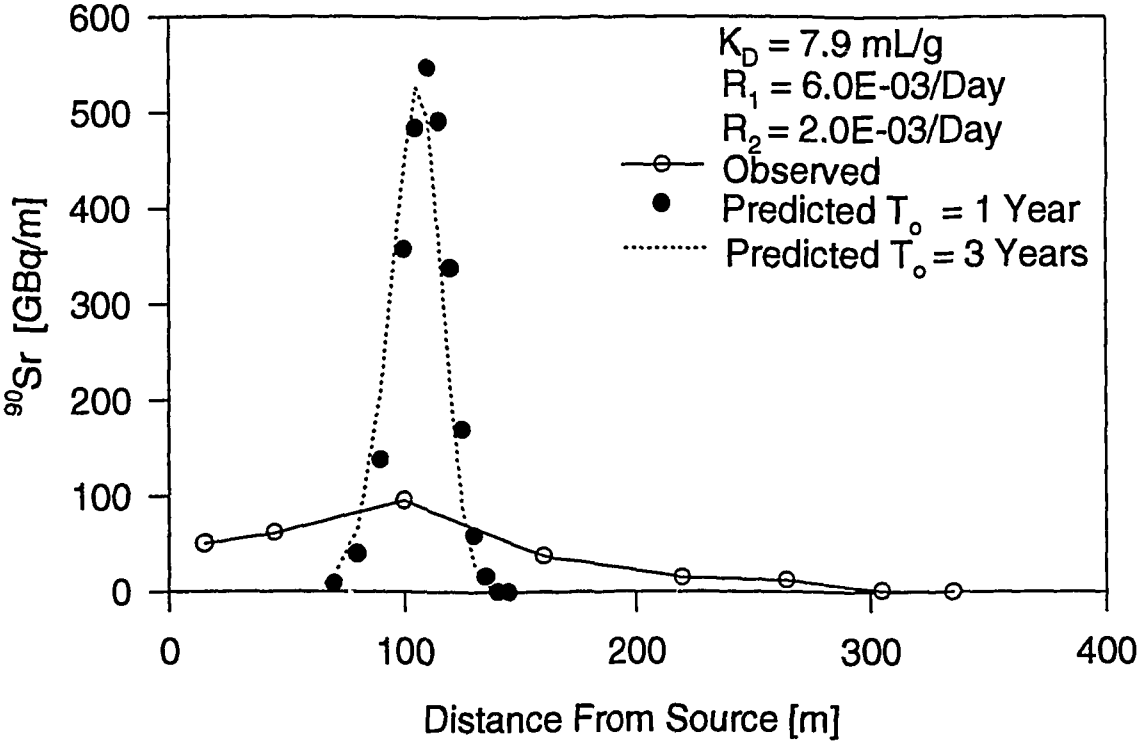

Figure 30 Predicted and observed ^{90}Sr activity profiles. Top - Field experiment derived rate constants and source term duration of one- and three-years. Bottom - Column experiment derived rate constants and source term duration of one- and three-years.

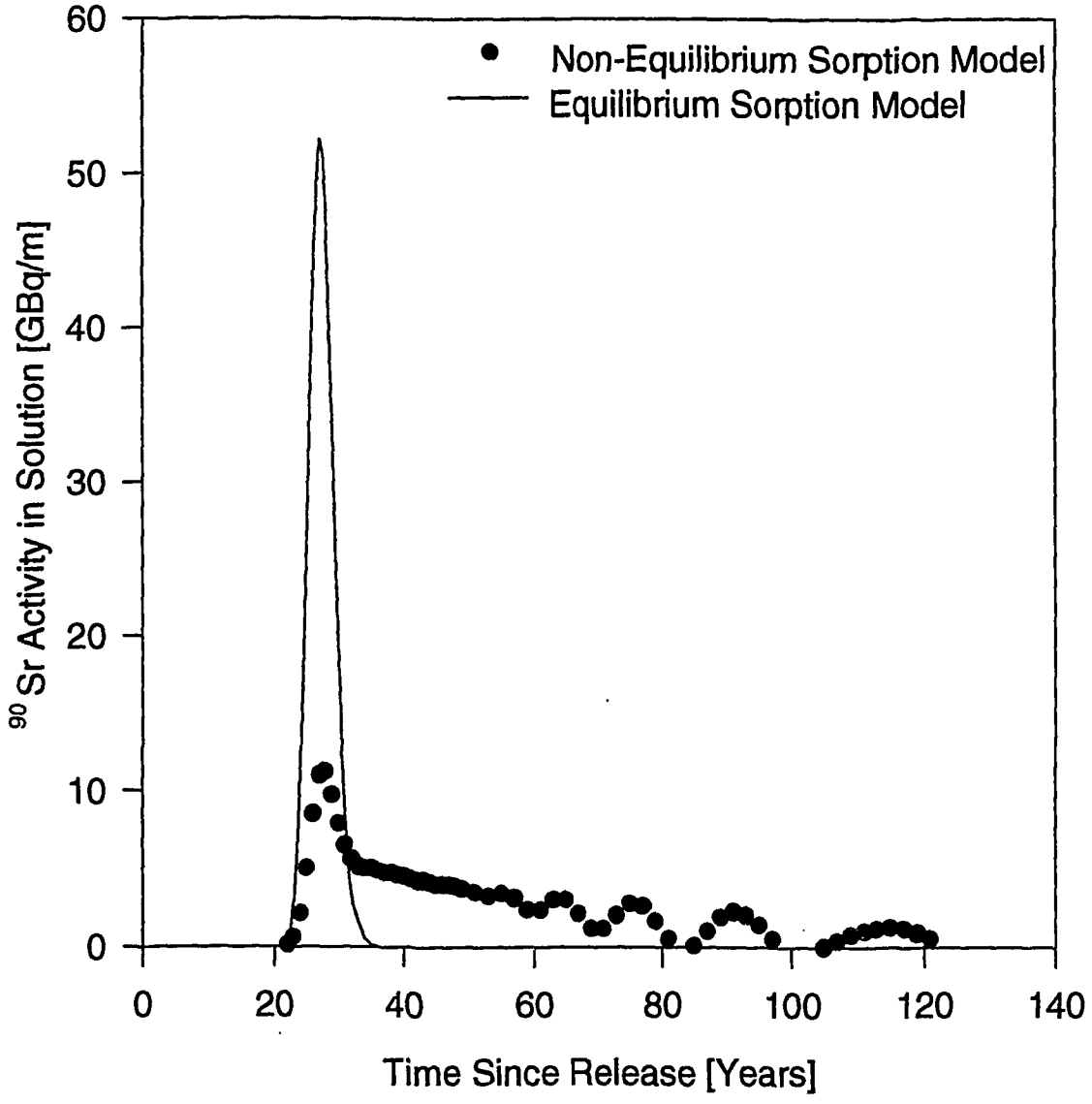

Figure 31 Predicted ^{90}Sr concentration-time curves at 110 m from the source for equilibrium and non-equilibrium sorption models

Cat. No. /No de cat.: CC2-11330E
ISBN 0-660-16205-9
ISSN 0067-0367

To identify individual documents in the series, we have assigned an AECL- number to each.

Please refer to the AECL- number when requesting additional copies of this document from:

Scientific Document Distribution Office (SDDO)
AECL
Chalk River, Ontario
Canada K0J 1J0

Fax: (613) 584-1745 Tel.: (613) 584-3311
ext. 4623

Price: B

Pour identifier les rapports individuels faisant partie de cette serie, nous avons affecté un numéro AECL- à chacun d'eux.

Veuillez indiquer le numéro AECL- lorsque vous demandez d'autres exemplaires de ce rapport au:

Service de Distribution des Documents Officiels
EACL
Chalk River (Ontario)
Canada K0J 1J0

Fax: (613) 584-1745 Tél.: (613) 584-3311
poste 4623

Prix: B